USER CLUSTERING IN MULTI CELLULAR MILLIMETER WAVE NOMA SYSTEMS

by

Ahmet Ersel Tuncer

B.S., Electrical and Electronics Engineering, Bilkent University, 2015

Submitted to the Institute for Graduate Studies in
Science and Engineering in partial fulfillment of
the requirements for the degree of
Master of Science

Graduate Program in Electrical and Electronics Engineering

Boğaziçi University

2020

ACKNOWLEDGEMENTS

I would first like to thank my thesis advisor Prof. Emin Anarım for supporting me throughout the graduate program from the beginning. His support was significant for this work to be completed. I am also sincerely grateful to my committee member Prof. Mutlu Koca, since he guided me in the right the direction whenever he thought I needed it. I would also like to thank my committee member Prof. Erdal Panayırcı for his valuable guidance and profound knowledge.

I would like to thank my friend and colleague Mustafa, as he took significant interest in quick brain storming sessions with me when it is needed. I am grateful to my friend Abdullah. I am also thankful to my company and my managers for encouraging me to study in a graduate program.

Finally and most importantly, I must express my sincere gratitude to my family for their love, support and encouragement throughout my years of study in the graduate program and during the completion of this work. My parents were always there for me and my brother. This work could not be completed without them. Thank you.

ABSTRACT

USER CLUSTERING IN MULTI CELLULAR MILLIMETER WAVE NOMA SYSTEMS

Nonorthogonal multiple access (NOMA) suffers from intra-beam interference in addition to inter-beam interference. Therefore, its performance is highly interference limited. However, implementation of NOMA on millimeter wave systems promises to overcome this issue. Intra-beam and inter-beam interference are diminished respectively by high path loss and directional beam characteristics of millimeter waves. Consequently, higher system output can be achieved by combining NOMA and the millimeter wave communications. Nonetheless, inter-cell interference should also be taken into consideration as mobile networks have a tendency to be denser with each new generation of mobile communication systems. Especially in millimeter wave systems, cell ranges are fairly smaller than conventional systems. User clustering and power allocation methods can be used effectively to diminish the negative impact of the interference. In this work, user clustering in multi cellular downlink millimeter wave NOMA systems is investigated. K-medoids, an unsupervised machine learning algorithm is used to cluster users with the goal of maximizing the system output while keeping the total transmission power and quality of service (QoS) constraints in consideration. The simulation results show that K-medoids user clustering successfully clusters physically pre-clustered users and increases the system output in comparison to several other user clustering methods. Additionally, performance improvement over traditional orthogonal multiple access (OMA) is also demonstrated.

ÖZET

ÇOK HÜCRELİ MİLİMETRE DALGA DİKGEN-OLMAYAN ÇOKLU ERİŞİM (NOMA) SİSTEMLERİNDE KULLANICI KÜMELEME

Dikgen-olmayan çoklu erişimin (NOMA) performansı, demetler arası girişime ek olarak demet içi girişimden dolayı da zarar görmektedir. Dolayısıyla performans, yüksek oranda girişim sınırlıdır. Fakat NOMA'nın milimetre dalga sistemlerinde kullanımı, bu sorunun çözümü konusunda oldukça umut vermektedir. Demet içi ve demetler arası girişim, milimetre dalgaların sırasıyla yüksek yol kaybı ve yönlü demet nitelikleri sayesinde zayıflamaktadır. Bu sebeple, milimetre dalga iletişimi ile NOMA birlikte kullanılarak daha yüksek performans hedefleri ulaşılabilir kılınabilmektedir. Mobil ağların her yeni nesil mobil iletişim sistemiyle beraber daha fazla yoğunlaşma eğilimi göz önüne alındığında, hücreler arası girişimin de hesaba katılması gerekmektedir. Özellikle milimetre dalga sistemlerinde hücre menzilleri, geleneksel sistemlerle karşılaştırıldığında oldukça küçüktür. Kullanıcı kümeleme ve güç paylaştırma metotlarını kullanarak girişimin olumsuz etkileri etkin bir şekilde hafifletilebilir. Bu tez çalışmasında, çok hücreli milimetre dalga aşağı yönlü NOMA sistemlerinde kullanıcı kümelemenin performansa etkisi incelenmektedir. Bir gözetimsiz makine öğrenimi algoritması olan K-medoids, kullanıcı kümeleme yöntemi olarak kullanılmıştır. Bunu yaparken, iletime ayrılan toplam güç ve kullanıcı hizmet kalitesi gibi kısıtları göz önünde bulundurarak sistem performansını azami seviyeye çıkarmak amaçlanmıştır. Elde edilen simulasyon sonuçlarına göre, K-medoids kullanıcı kümeleme yöntemi önceden fiziksel olarak kümelenmiş kullanıcıları başarıyla kümelemiştir ve karşılaştırılan diğer birkaç yönteme göre sistemin performansını yükseltmiştir. Buna ek olarak, NOMA sayesinde dikgen çoklu erişimin (OMA) üzerine eklenen kazanç da gözlenmiştir.

TABLE OF CONTENTS

LIST OF FIGURES

LIST OF SYMBOLS

$\mathbf{a_{BS}}(.)$, $\mathbf{a}(.)$	Steering vector
$\mathbf{a_{UE}}(.)$	Array response vector at user equipment
$\mathcal{B}$	Index set of base stations
B	Number of base stations
$\mathbb{C}$	Set of complex numbers
$\mathcal{C}$	Set of clusters
$\mathcal{CN}(\mu_x, \sigma_x^2)$	Complex Gaussian random variable with mean μ_x and variance σ_x^2
C_k	Set of users in cluster $k \in \mathcal{K}$
$d_{b,u}$	Distance between user $u \in \mathcal{U}$ and base station $b \in \mathcal{B}$
$d(.,.)$	Distance function for features
D	Antenna spacing of the base stations
$e_{b,u}$	AoD estimation error of base station $b \in \mathcal{B}$ for user $u \in \mathcal{U}$
$E\{.\}$	Expectation operator
$F_M(.)$	M-th order Fejér kernel
$g_{k,u}$	Equivalent channel gain of user $u \in C_k$ where $k \in \mathcal{K}$
$\tilde{g}_{k,u}$	Effective channel gain of user $u \in C_k$ where $k \in \mathcal{K}$
$\mathbf{h}_{b,u}$	Millimeter wave channel vector of user $u \in \mathcal{U}$ with respect to base station $b \in \mathcal{B}$
$\mathcal{K}$	Index set of clusters
K	Number of clusters
$\log(.)$	Logarithmic operator with base 2
$\mathcal{L}$	Index set of paths
L	Number of total paths
L_k	Number of users in cluster $k \in \mathcal{K}$
$\mathcal{M}$	Index set of transmitting antennas in the base stations
M	Number of transmitting antennas in the base stations
n_u	Complex i.i.d. additive Gaussian noise at user $u \in \mathcal{U}$

$\mathcal{N}$	Index set of receiving antennas in the user equipment
$\mathcal{N}(\mu_x, \sigma_x^2)$	Gaussian random variable with mean μ_x and variance σ_x^2
N	Number of receiving antennas in the user equipment
$\mathbf{p}$	Inter-cluster power allocation coefficient vector
p_k	Inter-cluster power allocation coefficient of cluster $k \in \mathcal{K}$
P	Total transmission power of the base stations
r	Radius of children distribution
R	Radius of parent distribution
R_{sum}	Sum rate
$s_{k,u}$	Transmitted message for user $u \in C_k$ where $k \in \mathcal{K}$
s_k	Superposition of $s_{k,u}$ for $\forall u \in C_k$ where $k \in \mathcal{K}$
u^k	Cluster-head or medoid user of cluster $k \in \mathcal{K}$
$u^{'}$	A user that interferes user $u \in C_k$ where $u^{'} \in C_l$ and $l \neq k$ for any $l, k \in \mathcal{K}$
$\mathcal{U}$	Index set of users
U	Number of users
U^*	Optimal value of sum rate maximization problem
$\bar{U}$	Optimal value of sum rate maximization problem with the minimum intra-cluster power allocation
U_k	Coalition utility
U_k^r	Coalition utility for proposal rejection
U_k^a	Coalition utility for proposal acceptance
$\mathbf{w}_{b,k}$	Beamforming vector formed at base station $b \in \mathcal{B}$ towards cluster $k \in \mathcal{K}$
$\mathbf{x}$	Feature vector
$y_{k,u}$	Received signal at user $u \in C_k$ where $k \in \mathcal{K}$
$\alpha_{u,l}$	Complex gain of l-th path of user $u \in \mathcal{U}$
α_u	Complex gain of LOS path of user $u \in \mathcal{U}$
$\boldsymbol{\beta}_k$	Intra-cluster power allocation coefficient vector of cluster $k \in \mathcal{K}$
$\bar{\boldsymbol{\beta}}_k$	Minimum intra-cluster power allocation coefficient vector of cluster $k \in \mathcal{K}$

$\tilde{\boldsymbol{\beta}}_k$	Excess intra-cluster power allocation coefficient vector of cluster $k \in \mathcal{K}$
$\beta_{k,u}$	Intra-cluster power allocation coefficient of user $u \in C_k$ where $k \in \mathcal{K}$
$\bar{\beta}_{k,u}$	Minimum intra-cluster power allocation coefficient of user $u \in C_k$ where $k \in \mathcal{K}$
$\tilde{\beta}_{k,u}$	Excess intra-cluster power allocation coefficient of user $u \in C_k$ where $k \in \mathcal{K}$
$\gamma_{b,u,l}$	Normalized AoA of path $l \in \mathcal{L}$ between user $u \in \mathcal{U}$ and base station $b \in \mathcal{B}$
$\Gamma_{k,u}$	SINR of user $u \in C_k$ where $k \in \mathcal{K}$
$\bar{\Gamma}_{k,u}$	SINR Threshold of user $u \in C_k$ where $k \in \mathcal{K}$
$\bar{\Gamma}$	Global SINR Threshold
ϵ	CSI Accuracy
$\zeta_{b,k}$	Normalized AoD between medoid of cluster $k \in \mathcal{K}$ and base station $b \in \mathcal{B}$
$\eta_{u,l}$	Path loss exponent of path $l \in \mathcal{L}$ of user $u \in \mathcal{U}$
η, η_{LOS}	Path loss exponent of LOS path
η_{NLOS}	Path loss exponent of NLOS path
θ	Angle of departure
$\theta_{b,u}$	AoD between user $u \in \mathcal{U}$ and base station $b \in \mathcal{B}$
$\hat{\theta}_{b,u}$	Estimated AoD between user $u \in \mathcal{U}$ and base station $b \in \mathcal{B}$
λ	Wavelength
π_k	Decoding order of SIC in cluster $k \in \mathcal{K}$
$\pi_k(j)$	User with the j-th decoded message in cluster $k \in \mathcal{K}$
σ^2	Noise power
ϕ	Normalized AoD
$\phi_{b,u,l}$	Normalized AoD of path $l \in \mathcal{L}$ between user $u \in \mathcal{U}$ and base station $b \in \mathcal{B}$
$\phi_{b,u}$	Normalized AoD of LOS path between user $u \in \mathcal{U}$ and base station $b \in \mathcal{B}$
$\psi(k)$	Base station serves to cluster $k \in \mathcal{K}$
$\forall$	For all

$\{.\}^H$	Hermitian of a matrix
$\|.\|$	Absolute value

LIST OF ACRONYMS/ABBREVIATIONS

AoD	Angle of Departure
CSI	Channel State Information
DoF	Degree of Freedom
EM	Expectation Maximization
HDTV	High Definition Television
i.i.d.	Independent and Identically Distributed
IoT	Internet of Things
LAB	Linear Approximate BUILD
LOS	Line-Of-Sight
MIMO	Multiple-Input and Multiple-Output
MISO	Multiple-Input and Single-Output
MRT	Maximum Ratio Transmission
NLOS	Non-Line-Of-Sight
NOMA	Nonorthogonal Multiple Access
OMA	Orthogonal Multiple Access
PAM	Partitioning Around Medoids
SINR	Signal-To-Interference-Plus-Noise Ratio
UHTV	Ultra-High Definition Video
ULA	Uniform Linear Array

1. INTRODUCTION

Technology evolves according to the needs of people and it becomes an inseparable part of their lives as it assists them. In time, further progress is required as the technology becomes a standard to the modern life. Mobile communications is an example of this tendency as there is an exponential growth in mobile traffic rates. The first generation of mobile communication systems supported only voice and text communication. Nowadays, mobile communications can provide communication types of higher data rates such as video. It also provides higher data rates overall due to increase in not only number of served user equipment but also the use of increasing number of internet services. The trend is expected to continue due to new emerging technologies. For example, number of served user equipment is predicted to increase drastically due to internet of things (IoT), in which equipment communicate without the need of any human interaction. On the other hand, newer services with higher data rates such as high definition television (HDTV) and ultra-high definition video (UHTV) requires higher throughput per device. For both cases of IoT and HDTV/UHTV, higher traffic volume is also required. Therefore, main requirements of the next generation of mobile communications can be expressed as higher traffic volume, higher area spectral efficiency and higher throughput per device. These requirements can be fulfilled by several ways. Firstly, larger bandwidths are required to increase the traffic volume. Current technology provides capacities close to Shannon Limit and conventional micro wave communications provide around 1-2 GHz available bandwidth [1]. The available bandwidth is considered low in the light of the expected increase in mobile traffic. Secondly, radio access points with smaller ranges increase traffic volume and area spectral efficiency by allowing more frequency reuse especially in urban areas. These radio access points are called small cells. Thirdly, more antennas in transmitting and receiving sides increases spectral efficiency and provides higher throughput. Millimeter wave communications combined with nonorthogonal multiple access (NOMA) and multiple-input and multiple-output (MIMO) is considered to be a solution to the requirements by enhancing communications in the mentioned three aspects.

1.1. Millimeter Waves

Electromagnetic waves are defined as the waves travel through space in the electromagnetic field. As they have distinct features with respect to their frequencies and wavelengths, they are categorized in the electromagnetic spectrum accordingly. The electromagnetic spectrum ranges from below 1 Hz to above 10^{25} Hz. This range is so large such that it corresponds to down from atomic distances up to thousands of kilometers in terms of wavelength. The frequency range is categorized into separate bands with different names. In terms of mobile communications, we are interested in radio waves. The electromagnetic spectrum is demonstrated in Figure 1.1. The millimeter waves are highlighted with the red crosshatching in the figure.

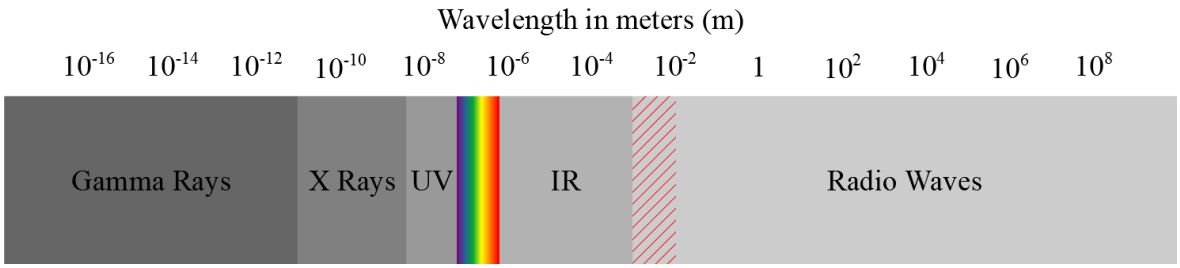

Figure 1.1. Electromagnetic Spectrum.

Millimeter waves are firstly studied more than 100 years ago. However, millimeter wave communications can be traced back to 1980s and early 1990s. In the recent years, study of millimeter wave communications has been accelerated due to the mentioned requirements of 5G. There are numerous projects and applications that support this process such as European Union initiated Millimetre-wave evolution for backhaul and access (MiWEBA), Beyond 2020 heterogeneous wireless networks with millimeter wave small cell access and backhauling (MiWaves) and millimeter wave based mobile radio access network for fifth generation integrated communications (mmMAGIC). Additionally, manufacturers of mobile communication devices such as Huawei and Ericsson also cooperate with mobile communication operators to test real life applications of millimeter wave communications [2].

Microwaves generally correspond to frequencies between 300 MHz and 30 GHz. Conventionally, microwave communications use the band below 6 GHz in which about bandwidth of 2 GHz is available [1]. Although microwaves have convenient propagation characteristics for mobile communications, the insufficient amount of bandwidth to be able to support the high data rate requirements of the next generation of mobile communications is a significant disadvantage. On the other hand, millimeter wave communications corresponds to frequencies between 30 GHz and 300 GHz. Consequently, it provides a much larger, currently unused bandwidth when it is compared to conventional microwave communications. Although it has unusually higher attenuation in some specific frequencies due to oxygen and water vapor absorption, millimeter wave communications can provide approximately 100 GHz of new spectrum by assuming the 40% availability for the bandwidth between 30 GHz and 300 GHz [1]. Therefore, it can achieve higher data rates.

As millimeter waves have shorter wavelength than micro waves, they have different characteristics. Firstly, millimeter waves have a much shorter range since they suffer from higher path loss. Therefore, they are perfectly suited in small cell applications since their smaller range decreases the inter-cell interference. Small cells are expected to be more favorable in urban areas in the next generation of mobile communications system because denser population of urban causes higher mobile traffic demand per area. Consequently, millimeter wave communications also are considered favorable due their compatibility with the dense networks.

The second characteristic of the millimeter waves is the higher penetration loss. Therefore, they are more susceptible to blockages from walls, buildings and furniture. Additionally, they have more attenuation due to atmospheric events such as rain or fog. Thus, the line-of-sight (LOS) signal has much lesser attenuation than the non-line-of-sight (NLOS) signal. According to [3], gain of the LOS path is nearly 20 dB stronger than gain of the NLOS paths. With these characteristics in consideration, significance of LOS signal is greater in millimeter wave applications than the conventional microwave systems.

Fortunately, the final characteristic of the millimeter waves is the fact that they are highly directional with narrower beamwidths and side lobes. Therefore, inter-cluster interference between beams is prevented from limiting capacity and beams can be aimed towards the cluster of users. Additionally, it provides better security and privacy against jamming and eavesdropping. Highly directional beams with high mobile traffic rate provide another possible application of millimeter wave communications, the wireless LOS backhauling between small cells. This application can be a financially favorable alternative to conventional backhauling. In addition, combination of millimeter wave backhauling with wireless optical backhauling can result in a more robust solution by eliminating the susceptibility to atmospheric events.

In this work, a millimeter wave model with only LOS component is implemented in order to simplify the calculations. No blockage is assumed. Further information about the implemented millimeter wave model is described in Section 2.2.

1.2. MIMO

The communication link between a transmitter and a receiver can be categorized according to number of antennas in each side. Single-input and single-output (SISO) is the simplest technique with one antenna at the transmitter and one antenna at the receiver. Single-input and multiple-output (SIMO), multiple-input and single-output (MISO) and MIMO follow as the remaining techniques. Increasing the number of antennas at the either side has advantages in terms of performance, data rates, inter-symbol interference (ISI) suppression and inter-user interference suppression.

MIMO provides higher spectral efficiency, energy efficiency and link reliability by using multiplexing, diversity and array gains. Spatial multiplexing is transmitting independent information streams in parallel through the channels with path gains that fade independently and it increases the data rate [4]. It is particularly beneficial in high signal-to-interference-plus-noise ratio (SINR) systems. The maximum number of channels is limited to the lesser in the number of antennas at the transmitter or receiver.

On the other hand, diversity is transmitting identical information through different paths which results in an increase in the link reliability. Therefore, there is a trade-off between multiplexing and diversity gains such that they cannot be simultaneously benefited in maximum. The cost of benefits of MIMO is the cost of the additional antennas, the space required for the additional antennas and the extra complexity for multi-dimensional signal processing [5]. Millimeter waves compensate the cost of the additional antennas and the space required for them since it requires physically smaller antennas due to the shorter wavelength.

A MIMO system with much larger number of antennas is called massive MIMO. Millimeter waves are also well suited for massive MIMO since they allow smaller antenna size as emphasized before. Antenna arrays with large number of antennas can be packed in a much smaller size with reduced cost and energy consumption such that user equipment can also be equipped with multiple antennas. Therefore, higher spectral efficiency can be achieved. Additionally, higher beamforming gain with massive MIMO can be exploited to enlarge the cell range [1].

In this work, base stations are assumed to have relatively small in number, yet multiple antennas. On the other hand, user equipment is presumed to have only one antenna in order to simplify the calculations. Although MISO is used in the simulations, the results can also be projected in MIMO case.

1.3. NOMA

Multiple access techniques generally use time, frequency and code domains to serve multiple users. For instance, frequency division multiple access (FDMA), time division multiple access (TDMA) and orthogonal frequency division multiple access (OFDMA) are conventional orthogonal multiple access (OMA) techniques. On the other hand, a new kind of multiple access technique called NOMA is in consideration for future mobile communication generations. NOMA differs from OMA by supporting higher number of users than the number of orthogonal resource channels.

It can be divided into two main categories as power-domain NOMA and code-domain NOMA. For the rest of the paper, NOMA refers to the power-domain NOMA and the latter is simply out of the scope.

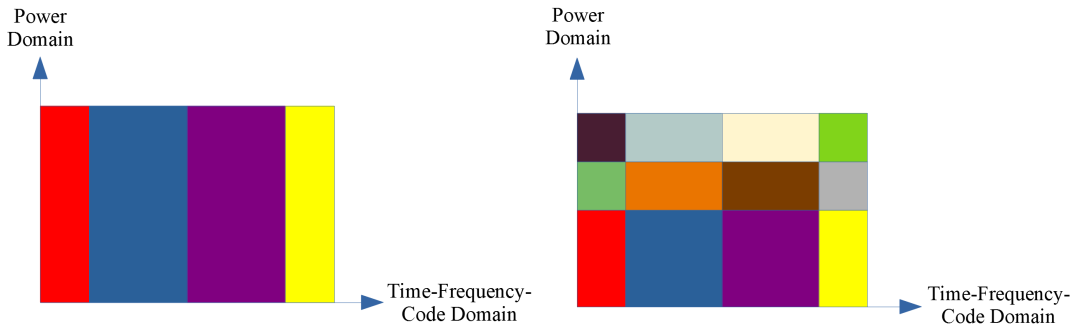

(a) OMA (b) NOMA

Figure 1.2. Domain Utilization for OMA and NOMA schemes.

NOMA brings power domain to use for multiple access and provides service to different users that share the same degrees of freedom (DoF) through superposition [6]. In other words, multiple users share the same time-frequency resources where their messages are superimposed on each other on the power domain. It is demonstrated on Figure 1.2. All users except the one with the lowest SINR are required to perform successive interference cancellation (SIC) in order to retrieve their messages from the received superimposed signal. Therefore, NOMA provides better spectral efficiency than OMA systems at the cost of an increased receiver complexity. It promises low latency, high reliability, massive connectivity, improved fairness, high throughput and high capacity [6]. Capacity increase and massive connectivity is provided since number of users served simultaneously is no longer limited to orthogonal resource channels. Additionally, serving users on the same DoF with different quality of service levels leads to low latency and improved fairness [6].

NOMA has intra-cluster interference in addition to inter-cluster interference compared to OMA. Therefore, interference is a stronger limiting factor to NOMA applications. Combination of NOMA and millimeter waves is perfectly suitable in order to overcome these problems and it has recently started to attract attention. High path loss of millimeter waves reduces the intra-cluster interference in NOMA [6].

Additionally, directional beams of millimeter waves diminish the inter-cluster interference. Therefore, the mobile traffic rate requirements can be fulfilled by combining NOMA and the millimeter waves, especially in urban areas. The symbiotic relationship between small cells, millimeter waves and NOMA is summarized in Figure 1.3.

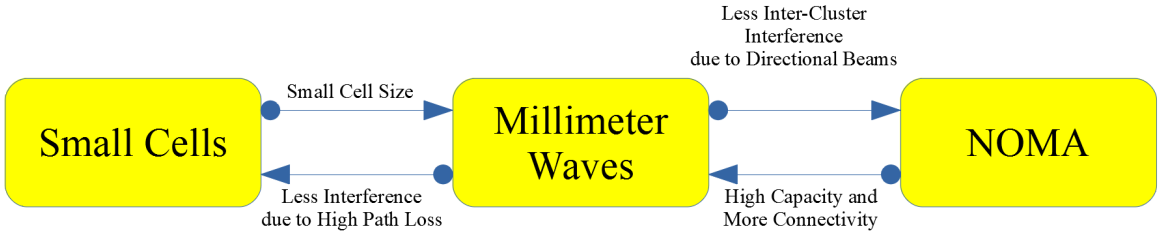

Figure 1.3. Relationship Between Small Cell Networks, Millimeter Wave Communications and NOMA.

Implementation of NOMA differs from OMA in terms of two aspects. Firstly, NOMA signal model includes the intra-cluster interference. Secondly, NOMA requires additional intra-cluster power allocation. Further information about signal model and power allocation is described in Section 2.3 and Chapter 5, respectively.

1.4. Literature Review

Millimeter wave NOMA systems recently gained a lot of popularity due to its promising features. There are many papers that investigate its performance with different beamforming, power allocation or user clustering algorithms in different simulation conditions. Specifically in this work, user clustering in multi cellular downlink millimeter wave NOMA systems is evaluated.

A user clustering algorithm for millimeter wave NOMA systems is initially evaluated in a simulation with single cell. This kind of simulation environment clearly demonstrates performance of the algorithm with respect to inter-cluster interference. User clustering problem is defined jointly with power allocation problem in [7], as a Stackelberg game based optimization problem in a system with minimum QoS constraints. The optimization problem consists of a leader problem and a follower problem.

The leader problem is chosen as the overall sum rate maximization of the system subject to user clustering and a sequential game based user clustering algorithm is designed as its solution. Single-antenna users are distributed around a base station with multiple antennas. The algorithm predetermines several users as cluster-heads such that the number of cluster-heads equals to the number of radio frequency (RF) chains. Then, it forms beams towards the cluster-heads. In conclusion, it is claimed that the algorithm improves the sum rate and reduces the outage probability. An adaptation of the algorithm is implemented in this work as it is described in Section 4.2.

Due to correlation features of users' spatial distributions in millimeter wave NOMA systems, user clustering with unsupervised machine learning methods has started to attract attention. It is offered in [8] to use unsupervised machine learning to cluster users with single antenna in a single millimeter wave NOMA cell with multiple transmitting antennas and minimum QoS constraints in order to maximize the sum rate. The authors particularly use a K-means based user clustering algorithm. Additionally, they offer an online version of the algorithm and evaluate it in a system with increasing number of users over time. It is concluded that the proposed algorithms enhance the system performance in both cases.

The sum-rate maximization problem in a downlink millimeter wave NOMA system is investigated in [9] and an expectation maximization (EM)-based algorithm for user clustering is proposed where EM is another unsupervised learning method. Additionally, an online EM-based clustering algorithm is offered and it is simulated in a very dynamic environment which includes user reduction, user increment and user movement options. It is concluded that the proposed algorithms increase the system performance in both cases.

Another unsupervised machine learning method, K-mediods is suggested in [10] in order to cluster users as an alternative to K-means algorithm. Both of the algorithms are very similar to each other. The main difference is the fact that data points are chosen as cluster centers in K-medoids in contrast to the K-means algorithm.

The authors study a completely different case with the application of simultaneous wireless information and power transfer (SWIPT) to areal millimeter wave NOMA systems. In this case, the aerial base station sends not only information but energy using NOMA to multiple single-antenna devices that decode information or harvest energy. The aim is to maximize the harvested energy with respect to some QoS constraints. The K-medoids algorithm has several realizations. In this case, it is realized by using partitioning around medoids (PAM) algorithm. Cartesian coordinates of users are used as features. In conclusion, it is claimed that the algorithm improves the performance in terms of the mentioned criteria. A K-medoids algorithm is also implemented in this work. Further information on the implemented K-medoids user clustering algorithm can be found in Section 4.3.

Inter-cluster interference in a single cell is one side of the coin. The other side is inter-cell interference in a multi cellular environment. Although it does not include NOMA, a beam interference model and a low complexity beam interference suppression algorithm based on user clustering for multi cellular millimeter wave systems is proposed in [11]. Additionally, multi cellular cooperative transmission is adopted to suppress the interference further. The algorithm aims to prevent frequent beam switching by using a user clustering algorithm with double preset thresholds and to achieve the ideal system performance.

A multi cellular setup in a millimeter wave angle-domain NOMA with massive MIMO and minimum QoS constraints is examined in [12]. There are three base station with 60-degree sectors. The authors focus on the three adjacent sectors with strong interference. The aim of this work is to maximize the system sum rate by designing precoders and decoders. Two design strategies are proposed: joint optimization of precoders/decoders and cooperative NOMA. A user pairing algorithm for each of the design strategies is also offered such that the algorithms aim to pair a near user with a far user on the same DoF. The results suggest improved performance for both of the design strategies.

The effect of beam interference in multi cellular millimeter wave NOMA systems is investigated in [13]. Dynamic beam switching and static beam selection is proposed in order to coordinate the beams effectively. In addition to these solutions, an improved downlink multi user simultaneous transmission scheme that aims to guarantee minimum QoS constraints is introduced. It is concluded that the proposed schemes enhance the system performance.

1.5. Scope Of The Thesis

Mobile communication systems can be evaluated with respect to many aspects such as output data rate or energy efficiency. Energy efficiency of a system is not only important in terms of operation costs but also important in terms of carbon emissions and climate control. However, it will be out of scope since one of the goals of this work is to evaluate system performance with respect to its fulfillment of the high data rate requirements. The sum rate performance of millimeter wave NOMA systems can be affected by many factors, such as blockages, channel state information (CSI) perfection, intra-cluster, inter-cluster and inter-cell interference. The effects of these factors can be improved by methods of beamforming, user clustering, inter-cluster and intra-cluster power allocation. The main goal of this work is to evaluate user clustering in a multi cellular setup with respect to the system performance. Therefore, improvements on beamforming techniques and power allocation are out of the scope of this work.

Chapter 1 is the introductory chapter. Millimeter waves are introduced in Section 1.1, MIMO is summarized in Section 1.2, NOMA is explained in Section 1.3 and a brief literature review is presented in Section 1.4. The rest of the thesis is organized in six main chapters. The implemented system models are explained in detail in Chapter 2. The Chapter 2 is organized as follows: the correlated spatial distribution model is illustrated in Section 2.1, the single path millimeter wave channel model with only LOS in consideration is described in Section 2.2, the millimeter wave NOMA signal model and SINR calculations are summarized in Section 2.3, and the CSI imperfection model is expressed in Section 2.4. The user clustering algorithms are explained in Chapter 4.

The maximum ratio transmission (MRT) beamforming is presented in Chapter 3. The power allocation methods for both inter-cluster power allocation and intra-cluster power allocation are introduced in Chapter 5. The simulation environment is described in Chapter 6 and then the results are presented. The thesis is concluded in Chapter 7.

2. SYSTEM MODEL

Assume a downlink millimeter wave NOMA system with B base stations and U users. All base stations are assumed to have M transmitting antennas and all users are assumed to have N receiving antennas. Users are clustered into K clusters and each cluster is served simultaneously over a unique beam by following NOMA principles. Index sets of base stations, transmitting antennas, receiving antennas, users and clusters are $\mathcal{B} = \{1, 2, ..., B\}$, $\mathcal{M} = \{1, 2, ..., M\}$, $\mathcal{N} = \{1, 2, ..., N\}$, $\mathcal{U} = \{1, 2, ..., U\}$ and $\mathcal{K} = \{1, 2, ..., K\}$, respectively.

Initially, a correlated spatial distribution model will be introduced in this chapter. Then, a complex millimeter wave channel model will be simplified into a simpler form. Finally, the signal model and the CSI imperfection model will be described.

2.1. Spatial Distribution Model

In OMA, high channel correlation decreases the system throughput by reducing multiplexing gain. On the other hand, it is concluded in [14] that higher channel correlation with NOMA can acquire optimal system output for MIMO systems. Consequently, millimeter wave channel combined with NOMA is a suitable pair to improve overall system performance.

In this work, a correlated spatial distribution model is adopted in order to fully demonstrate the system performance of millimeter wave NOMA systems. Initially, $B = K$ is assumed for simplification so that the clusters are one-to-one matched with the base stations. K uncorrelated parent points are placed in the two dimensional space between the base stations such that they are on range R from their matched base stations. Then, users are independently and identically distributed (i.i.d.) around the parents within a certain radius r so that every user is an offspring of a parent. The distribution of children is often called the uniform spatial distribution.

They are usually distributed equally among the clusters in this work even though it is not necessary. The spatial distribution model is built around correlation of users' millimeter wave channel vectors, which will be described in the next section. It is simply illustrated in Figure 2.1.

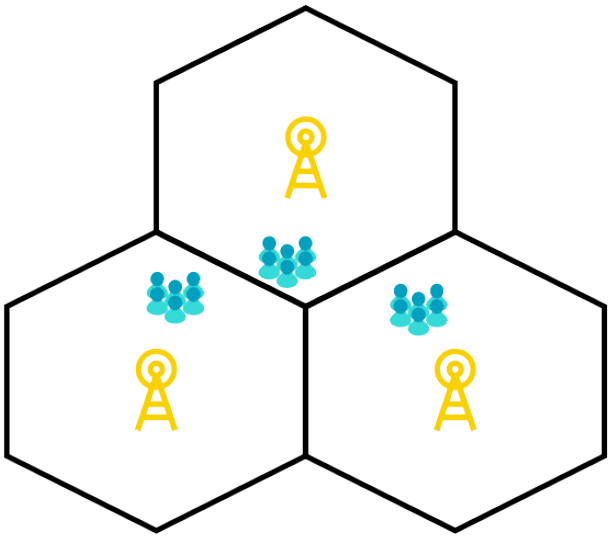

Figure 2.1. Illustration of the Multi Cellular Millimeter Wave NOMA Spatial Model.

2.2. Millimeter Wave Channel Model

A channel model represents characteristics of the channel. Millimeter wave channels has limited scattering due to high free-space path loss. Additionally, they are sparse in angular domain and highly correlated. Therefore, they have a very distinct channel model compared to the conventional macro wave channels. Channel models with different complexity levels can be utilized in order to represent the channel characteristics. In this section, a general millimeter wave channel model with a decent complexity is initially defined. Then, it is finalized in a much simpler form by making several assumptions.

A general model for millimeter wave channel vector of any user $u \in \mathcal{U}$ with respect to any base station $b \in \mathcal{B}$ can be expressed as

$$\mathbf{h}_{b,u} = \sum_{l=0}^{L} \sqrt[2]{M} \frac{\mathbf{a}_{UE}^{H}(\gamma_{b,u,l}) \mathbf{a}_{BS}(\phi_{b,u,l}) \alpha_{u,l}}{\sqrt[2]{(1 + d_{b,u}^{\eta_{u,l}})}}, \tag{2.1}$$

where $l \in \mathcal{L} = \{0, 1, ..., L-1\}$, $l = 0$ denotes the LOS path and L denotes the number of total paths. $d_{b,u}$ denotes the distance between the user u and the base station b. $\eta_{u,l}$ denotes the path loss exponent corresponding to the l-th path of the user u. The path loss exponent can be assumed as $\eta_{LOS} = 2$ and $\eta_{NLOS} = 3$ for all paths of users. $\alpha_{u,l} \sim \mathcal{CN}(0, 1)$ denotes the complex gain of the path l of the user u. $\phi_{b,u,l}$ is the normalized angle of departure (AoD) of the path l between the user u and the base station b. The normalized AoD is calculated by

$$\phi = \frac{2D \sin\theta}{\lambda}, \tag{2.2}$$

where $\theta \in [0, 2\pi]$ denotes AoD. Similarly, $\gamma_{b,u,l}$ is the normalized angle of arrival of the path l between the user u and base station b. The normalized angle of arrival is calculated similarly to the normalized AoD by (2.2). D denotes antenna spacing of the base station and λ denotes the wavelength. As a general rule, $\frac{D}{\lambda} \leq 0.5$ and it is assumed that $\frac{D}{\lambda} = 0.5$ in this work. $\mathbf{a}_{BS}(\phi_{b,u,l})$ denotes the steering vector of the path l between the user u and the base station b. Assuming the typical uniform linear array (ULA), the steering vector can be expressed as

$$\mathbf{a}_{BS}(\phi_{b,u,l}) = \frac{1}{\sqrt[2]{M}} \left[\; 1, \quad e^{-j\pi\phi_{b,u,l}}, \quad \cdots, \quad e^{-j\pi(M-1)\phi_{b,u,l}} \; \right]. \tag{2.3}$$

The array response vector at the user equipment, $\mathbf{a}_{UE}(\gamma_{b,u,l})$ can be written in a similar fashion, by using number of receiving antennas in user equipment instead of number of transmitting antennas of the base station. It should be noted that the general model for millimeter wave channel vector defined on (2.1) is similar to the ones in [15] and [16].

In this work, user equipment is assumed to have one receiving antenna each to simplify the calculations. Therefore, $\gamma_{b,u,l}$ and $\mathbf{a}_{UE}(\gamma_{b,u,l})$ are ignored and $\mathbf{a}_{BS}(\phi_{b,u,l})$ is denoted by $\mathbf{a}(\phi_{b,u,l})$ from this point on. Additionally, gain of the LOS path is nearly 20 dB stronger than gain of the NLOS paths [3]. As a result, NLOS paths are ignored in order to simplify the channel model in this work. In other words, $L = 1$ is assumed, similar to the models used in [8] and [17]. The resulting simplified single-path millimeter wave channel vector can be expressed as

$$\mathbf{h}_{b,u} = \sqrt[2]{M}\frac{\mathbf{a}(\phi_{b,u})\alpha_u}{\sqrt[2]{(1+d_{b,u}^{\eta})}}. \tag{2.4}$$

The millimeter wave channel vector is the essential feature to not only user clustering but also signal model. A successful user clustering requires users with correlated channel vectors to be clustered in the same cluster. On the other hand, SINR and sum rate calculations in the signal model include the channel vectors of the users. The signal model will be described in the next section.

2.3. Signal Model

The base stations send distinct messages to users. For OMA scheme, each beam carries a single message in the same orthogonal resource slot. On the other hand, beams carry multiple messages in superposition for NOMA scheme. Therefore, they have similar but different signal models such that the only difference is the intra-beam interference.

2.3.1. OMA Signal Model

In OMA, users in a cluster cannot communicate on the same orthogonal resource over the same beam and the only power allocation is the inter-cluster power allocation.

Let

$$\mathbf{p} = \left[\begin{array}{cccc} p_1, & p_2, & \cdots, & p_K \end{array} \right], \text{ where } \sum_{k=1}^{K} p_k \leq P \tag{2.5}$$

denote the inter-cluster power allocation and P is the total transmission power of the base stations. Let C_k refer to set of users in the k-th cluster where $k \in \mathcal{K}$ and $\mathcal{C} = \{C_1, ..., C_K\}$ denotes the set of clusters. Suppose $\psi(k)$ refers to the base station that serves to C_k. $s_{k,u}$ denotes the transmitted message for the user $u \in C_k$. $\mathbf{w}_{b,k} \in \mathbb{C}^{Mx1}$ denotes the beamforming vector that is formed at the base station b towards C_k. For OMA case, the received signal at the user $u \in C_k$, $y_{k,u}$, is given by

$$y_{k,u} = \mathbf{h}^H_{\psi(k),u} \sqrt{p_k} \mathbf{w}_{\psi(k),k} s_{k,u} + \sum_{l \neq k} \mathbf{h}^H_{\psi(l),u} \sqrt{p_l} \mathbf{w}_{\psi(l),l} s_{l,u'} + n_u, \tag{2.6}$$

where $n_u \sim \mathcal{CN}(0, \sigma^2)$ denotes the complex i.i.d. additive Gaussian noise at the u-th user where σ^2 is the noise power. Let $u^{'} \in C_l$ denote a user that interferes the user $u \in C_k$ over a different beam where $l \neq k$. The first term in (2.6) denotes the desired message and the second term is the interference caused from other beams. Decent user clustering, beamforming, inter-cluster power allocation or beam switching methods are required to diminish the second term. The SINR of user $u \in C_k$ can be calculated as

$$\Gamma_{k,u} = \frac{p_k |\mathbf{h}^H_{\psi(k),u} \mathbf{w}_{\psi(k),k}|^2}{\sum_{l \neq k} p_l |\mathbf{h}^H_{\psi(l),u} \mathbf{w}_{\psi(l),l}|^2 + \sigma^2}. \tag{2.7}$$

Then, the sum rate can be expressed as

$$R_{sum} = \sum_{k=1}^{K} E\{\log(1 + \Gamma_{k,u})\}, \text{ where } \forall u \in C_k. \tag{2.8}$$

2.3.2. NOMA Signal Model

Let L_k denote the cardinality of C_k where $\forall k \in \mathcal{K}$. $\pi_k(j)$ denotes the user with j-th decoded message of k-th cluster's SIC. Let

$$\boldsymbol{\beta}_k = \left[\begin{array}{cccc} \beta_{k,\pi_k(1)}, & \beta_{k,\pi_k(2)}, & \cdots, & \beta_{k,\pi_k(L_k)} \end{array} \right], \text{ where } \sum_{i=1}^{L_k} \beta_{k,\pi_k(i)} = 1, \forall k \in \mathcal{K} \tag{2.9}$$

denote the intra-cluster power allocation vector for the k-th cluster. The superposition of messages for the k-th cluster is denoted by $s_k = \sum_{u=1}^{L_k} \sqrt{\beta_{k,u}} s_{k,u}$. The received signal at the user $u \in C_k$ is given by

$$\begin{aligned} y_{k,u} = \mathbf{h}_{\psi(k),u}^H \sqrt{p_k} \mathbf{w}_{\psi(k),k} \sqrt{\beta_{k,u}} s_{k,u} + \mathbf{h}_{\psi(k),u}^H \sqrt{p_k} \mathbf{w}_{\psi(k),k} \sum_{v=1, v \neq u}^{L_k} \sqrt{\beta_{k,v}} s_{k,v} \\ + \sum_{l \neq k} \mathbf{h}_{\psi(l),u}^H \sqrt{p_l} \mathbf{w}_{\psi(l),l} s_l + n_u. \end{aligned} \tag{2.10}$$

The second term is the intra-cluster interference and it is eliminated by using decent a intra-cluster power allocation method and SIC. The SINR of user $\pi_k(j) \in C_k$ can be calculated from (2.10) as

$$\Gamma_{k,\pi_k(j)} = \frac{p_k \beta_{k,\pi_k(j)} |\mathbf{h}_{\psi(k),\pi_k(j)}^H \mathbf{w}_{\psi(k),k}|^2}{p_k |\mathbf{h}_{\psi(k),\pi_k(j)}^H \mathbf{w}_{\psi(k),k}|^2 \sum_{i>j} \beta_{k,\pi_k(i)} + \sum_{l \neq k} p_l |\mathbf{h}_{\psi(l),\pi_k(j)}^H \mathbf{w}_{\psi(l),l}|^2 + \sigma^2}. \tag{2.11}$$

Then, the sum rate can be expressed as

$$R_{sum} = \sum_{k=1}^{K} \sum_{j=1}^{L_k} \log(1 + \Gamma_{k,\pi_k(j)}). \tag{2.12}$$

In this work, the system performance is evaluated over the overall sum rate. Therefore, this section forms a significant basis for the simulation. The signal model considers the desired signal, interference and noise as factors to the performance. Another factor to the performance, CSI imperfection is described in the next section.

2.4. CSI Imperfection

CSI refers to state of the channel between a transmitter and a receiver. It continuously changes during the transmission. Perfect CSI knowledge at the receiver or the transmitter significantly affects the channel capacity. If CSI is only known at the receiver, the transmitter cannot dynamically adapt its transmission strategy according to the CSI. Consequently, it results in a lower capacity in fading channels than Additive White Gaussian Noise (AWGN) channels and the decrease can be significant if the receiver CSI is imperfect [18]. On the other hand, better channel capacity results can be reached if both the transmitter and receiver CSI is known since the transmitter can dynamically adapt power and resource allocation according to the CSI.

In the implemented millimeter wave NOMA system, the CSI is represented by the channel model vector on (2.4). Imperfect CSI at the base stations decreases the system output by affecting the performance of user clustering and power allocation. A non-optimal user clustering would result in misdirected beams and increased inter-cluster interference. Additionally, a non-optimal intra-cluster power allocation would increase the intra-cluster interference and decrease the SIC performance.

CSI can be regarded in two categories: AoD and the channel gain [19]. In this work, the main focus is user clustering by using K-medoids algorithm. Since AoD of users are used as the only features in the proposed algorithm, CSI imperfection will only be considered in terms of AoD in order to evaluate the user clustering algorithm with respect to CSI imperfection at the base stations. Imperfect CSI will be modeled such that $\hat{\theta}_{b,u}$, the estimated AoD of user u with respect to base station b is

$$\hat{\theta}_{b,u} = \epsilon\theta_{b,u} + \sqrt{1-\epsilon^2}e_{b,u}, \tag{2.13}$$

where $\theta_{b,u}$ is the actual AoD of user u with respect to base station b, $\epsilon \in [0,1]$ denotes the CSI accuracy, and i.i.d. $e_{b,u} \sim \mathcal{N}(0,1)$ denotes the AoD estimation error of the base station b for the user u.

In conclusion, the system model defines rules and models to initialize the system and run the simulation. Once the system is initialized, the next step before clustering users is to define a beamforming technique. In Chapter 3, the implemented beamforming technique presented.

3. BEAMFORMING

Beam misalignment can occur due to imperfect beamforming techniques, imperfect CSI and mobility of user equipment as it is stated in [1]. Hence, implementation of adaptive beamforming techniques is important to overcome the mentioned challenges and prevent any beam misalignment. In this work, performance of user clustering will be measured. Therefore, only one beamforming technique is implemented and the beams are one-to-one matched with the clusters in our simulations.

Beamforming can be simply categorized into three groups as analog, digital and hybrid beamforming. Analog beamforming performs poorly on millimeter wave communications and digital beamforming has more complex hardware requirements, higher cost and higher energy consumption [1]. On the other hand, hybrid beamforming has a performance near to the optimal case with more reasonable hardware requirements, cost and energy consumption [1]. Therefore, it is considered suitable in millimeter wave communication systems. MRT beamforming is implemented in this work such that

$$\mathbf{w}_{\psi(k),k} = \mathbf{a}(\zeta_{\psi(k),k}), \tag{3.1}$$

where $\zeta_{\psi(k),k}$ corresponds to the normalized AoD for the k-th cluster from the base station $\psi(k)$. It should be noted that $|(\mathbf{w}_{\psi(k),k})_i|$ is constant for $\forall i \in \mathcal{M}$ since it is implemented using analog shifters.

The effective channel gain of the user $u \in C_k$ is

$$\tilde{g}_{k,u} = |\mathbf{h}^H_{\psi(k),u}\mathbf{w}_{\psi(k),k}|. \tag{3.2}$$

The term $|\mathbf{a}(\phi_{\psi(k),u})^H\mathbf{a}(\zeta_{\psi(k),k})|$ in (3.2) plays a key role to give a metric of similarity between a user's channel vector and a beam where $\mathbf{a}(\phi_{\psi(k),u})$ is the steering vector of the user u, $\phi_{\psi(k),u}$ is the AoD of the user u and $\mathbf{a}(\zeta_{\psi(k),k})$ represents the formed beam.

In [3], it is stated that the inner product represents the beam pattern for the beam $\mathbf{a}(\zeta_{\psi(k),k})$ and it can also explicitly expressed by

$$\begin{aligned} |\mathbf{a}(\phi_{\psi(k),u})^H \mathbf{a}(\zeta_{\psi(k),k})| &= \frac{1}{M} \left| \sum_{n=0}^{M-1} e^{-j\pi n(\zeta_{\psi(k),k} - \phi_{\psi(k),u})} \right| \\ &\approx \frac{1}{M} F_M(\pi(\zeta_{\psi(k),k} - \phi_{\psi(k),u})). \end{aligned} \tag{3.3}$$

where F_M is called M-th order Fejér Kernel. $(\zeta_{\psi(k),k} - \phi_{\psi(k),u})$ denotes the difference between normalized AoD of the k-th beam and the user u. The Fejér Kernel can be visualized for different M values as in Figure 3.1 in order to demonstrate the effect of number of transmission antennas.

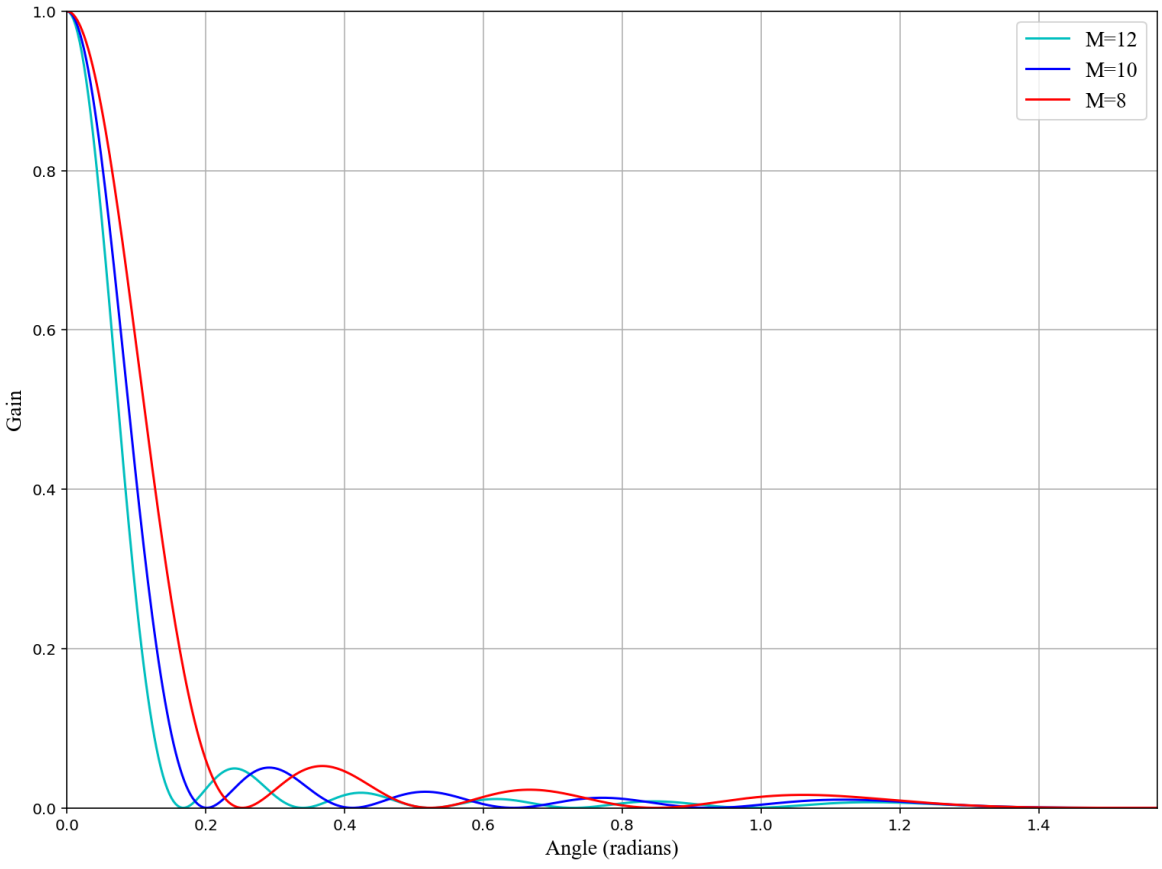

Figure 3.1. Beam Pattern for $M = 8, 10, 12$.

The Fejér Kernel gives the maximum value of one when the difference is zero. It has the standard beam pattern of ULAs where it forms the main lobe and the side lobes as the difference increases [3]. The pattern can be observed in Figure 3.1. Consequently, the main lobe gets wider as M decreases and visa versa. The wider main lobe increases inter-beam and inter-cell interference. On the other hand, a very thin beam may not serve all users in a wider cluster. Therefore, value of the number of antennas is significant to the system performance as it directly affects the beam pattern. The performance of randomly distributed beams in millimeter wave Multiple-Input and Single-Output (MISO) systems is investigated in [3]. The authors aim to have users such that the differences between their normalized AoDs and the normalized angle of their corresponding beams are sufficiently less than $1/M$ to achieve a good performance.

The beamforming vector defined in (3.1) requires one parameter: the normalized AoD for the cluster k from the base station b. In this work, user clustering methods forms clusters and pairs them to base station in a one-to-one manner. Therefore, the normalized AoD of the beams are also determined by user clustering methods, which are introduced in the next chapter.

4. USER CLUSTERING METHODS

A successful user clustering method for millimeter wave systems aims to cluster users such that users with correlated channels would be in the same cluster. It diminishes inter-cluster and intra-cluster interference and allows the fulfillment of QoS constraints due to the directionality characteristic of millimeter waves. Consequently, both OMA and NOMA scheme require a successful user clustering in order to perform optimally. The user clustering methods implemented in this work are random user clustering, sequential game based user clustering and K-medoids based user clustering. The reason for these methods to be chosen is to emphasize the effect of user clustering on the system performance. Random user clustering method is implemented to demonstrate the significance of a decent user clustering on the system performance, as it is expected to have the worst performance. On the other hand, sequential game based user clustering method is implemented to evaluate the performance of NOMA with a non-optimal method. Lastly, K-medoids based user clustering method is implemented to demonstrate the system performance with an optimal method.

As it is previously mentioned in the Section 2.1, users are distributed among K uncorrelated parent points. Consequently, the system aims to form K clusters where each user is an element of only one cluster, $C_i \cap C_j = \emptyset$ where $i \neq j, \forall i, j \in \mathcal{K}$. It is assumed that number of clusters cannot be bigger than number of transmitting antennas, $K \leq M$. The following sections describe each of the implemented methods in detail.

4.1. Random User Clustering Method

Randomly assigning users to clusters is assumed to have the worst system performance among the other implemented user clustering methods. It not only worsens the inter-beam interference but also the intra-beam interference, especially in NOMA. Therefore, random user clustering in NOMA is expected to perform worse than OMA.

The reason of its implementation in this work is to provide a lower limit for NOMA system performance and emphasize the significance of a dedicated user clustering method. It follows a uniform distribution and does not guarantee equal number of users for each cluster. On the other hand, it guarantees to form K clusters exactly. The random user clustering method is implemented such that the beams are aimed towards a random member of each cluster.

4.2. Sequential Game Based User Clustering Method

As mentioned in Section 1.4, user clustering and intra-cluster power allocation problems in downlink millimeter wave NOMA systems are jointly defined as a Stackelberg game-based optimization problem in [7]. The Stackelberg game-based optimization problem consists of a leader problem and a follower problem. The leader problem is chosen as maximizing the overall sum rate of the system subject to user clustering. On the other hand, the follower problem is chosen as maximizing the total sum rate of each cluster subject to intra-cluster power allocation. The optimal solutions for both of the problems are reached at the Stackelberg equilibrium.

A sequential game based user clustering algorithm is proposed in [7], as a solution the the leader problem. It has three phases: the initial phase, the proposal phase and the response phase. The algorithm is assumed to know the exact cluster number and unique cluster-head users for each cluster in its initial phase. Although knowing the exact cluster number is not presumed in this work, it is allowed for random and sequential game based user clustering methods since these algorithms are only implemented to provide a performance comparison for the proposed K-medoids user clustering method. Additionally, parent points are not implemented as users in this work. Therefore, there are no predetermined cluster-heads. The closest users to each base station are chosen as cluster-head users in the implemented sequential game based user clustering algorithm. The final step of the initial phase is to distribute other cluster member users randomly among the clusters. In the proposal phase, a cluster-head makes a new proposal to a user in a different cluster to join its cluster.

Initial Phase:

Cluster-head users are determined as the closest users to each base station and they form different cluster-base station pairs.

All other cluster members are determined randomly.

Proposal Phase:

for any cluster-head user u^k, where $k \in \mathcal{K}$, **do**

User u^k makes a new proposal.

Response Phase:

for any cluster member user u, where $u \notin C_k$, **do**

Calculate the coalition utility for proposal rejection, U_k^r.

User u leaves its current cluster and joins C_k temporarily.

Calculate the coalition utility for proposal acceptance, U_k^a.

if $U_k^r < U_k^a$ **then**

The proposal is accepted and User u leaves its current cluster and joins C_k permanently.

else

The proposal is rejected and User u stays in its current cluster.

end if

end for

end for

The game is stopped when no cluster member can accept any new proposal.

Figure 4.1. Sequential Game Based User Clustering Algorithm.

In this point, a pre-determined function called the coalition utility should be used to decide the outcome of the proposal. This phase is called the response phase. The similarity between two channels in view of base station b can be represented by $|\mathbf{a}(\phi_{b,u})^H \mathbf{a}(\phi_{b,v})|$ where $\mathbf{a}(\phi_{b,u})$ and $\mathbf{a}(\phi_{b,v})$ denote the steering vectors of user u and user v, respectively. As proven by (3.3), it is equivalent to $F_M(\phi_{b,u} - \phi_{b,v})$. The Fejér Kernel is maximum when the input $\phi_{b,u} - \phi_{b,v}$ equals to zero. It also converges to zero as the input increases. Therefore, the coalition utility, U_k can be defined by using normalized AoD's of users as

$$U_k = \frac{\sum_{u \in C_k} \left| \phi_{\psi(k),u} - \phi_{\psi(k),u^k} \right|}{L_k}, \tag{4.1}$$

where u^k denotes the cluster-head user of the k-th cluster. The proposal phase and the response phase iterates until no further proposal can be accepted. Lastly, the beams are aligned towards the cluster-head users. The algorithm is summarized in Figure 4.1.

4.3. K-Medoids Based User Clustering Method

Unsupervised machine learning algorithms do not require any labeled data and any training. K-medoids is one of them and it aims to group similar data points in a given number of clusters. In simple terms, a set of features and the desired number of clusters are given to the method as parameters and it clusters users such that the intra-cluster distances would be minimal. As mentioned before, users are pre-clustered physically in order to fully benefit from the characteristics of millimeter wave NOMA systems. Although most of the unsupervised machine learning methods would give similar results for the implemented spatial distribution model, K-means and K-medoids stand out as the simplest methods in terms of complexity. However, K-medoids is chosen as the proposed user clustering method in this work as it is more robust to outliers than K-means [20].

K-medoids method is usually referred as partitioning around medoids (PAM) since PAM is one of the most recognized algorithms to cluster using medoids [21].

There are newer and more optimized algorithms as alternatives to PAM, such as the algorithm proposed in [22] or the FastPAM algorithm proposed in [23]. As the newest one, the authors of [23] claim that it provides at least $O(K)$-fold speedup over PAM. Therefore, it is chosen as the algorithm to perform K-medoids based user clustering in this work.

K-medoids consists of two phases: the initialization and the execution. In the initialization phase, the initial medoids are determined. In [10], the medoids are initialized randomly. On the other hand, they can also be initialized more systematically, like the BUILD algorithm mentioned in [21]. In the execution phase, clustering is improved iteratively until a local optimum or maximum number of iterations is reached such as the SWAP algorithm in [21]. In [23], the initialization phase is switched with a newly proposed algorithm called linear approximate BUILD (LAB). LAB aims to initialize the medoids sufficiently good by using a relatively small sample set of users in order to provide lower complexity. However, the main factor to reduce the complexity is to prefer FastPAM in the execution phase. In FastPAM, distances between all users and their preferred medoids are cached initially. Euclidean square metric is used as the distance function in this work. Then, the algorithm determines the best swap operations for each medoid and performs the best swap among them in each iteration. It stops when the local optimum is reached. The algorithm is outlined in Figure 4.2.

Initialization Phase:
K medoids are initialized by using LAB.
Execution Phase:
while Local optimum for medoids or maximum number of iterations is not reached **do**
  Determine the best swap operations for each medoid.
  Perform the best swap operation among them.
end while

Figure 4.2. K-medoids Based User Clustering Algorithm.

Users with similar channel conditions should be clustered in the same cluster to be able to achieve higher system output. Therefore, features for the algorithm should reflect the channel conditions. As mentioned in Section 4.2, the normalized AoD's can be used as a feature for user clustering methods. Since B base stations are used in the simulation, AoD's to each base station can be used as a single feature, which sums up to B features per user. Unfortunately, it should be noted that the sharing of this information between the base stations increases the backhaul complexity. However, this type of communication is required in order to improve the system performance.

Another important parameter to K-medoids is the presumed number of clusters. There are several methods to predict the correct parameter such as silhouette, elbow method and Shadow statistics. The implemented method to determine the number of clusters is the elbow method [24]. In this method, K-medoids algorithm is run for a range of number of clusters values. The average internal cluster distance is calculated for each presumed value for number of clusters by using

$$W = \sum_{k=1}^{K} \sum_{u,u^k \in C_k} d(\mathbf{x}_u, \mathbf{x}_{u^k}), \tag{4.2}$$

where $\mathbf{x_u}$ denotes feature vector of the user u, u^k denotes the medoid user of the k-th cluster and $d(\mathbf{x}_u, \mathbf{x}_{u^k})$ denotes the distance function which is Euclidean squared distance in this case. The optimal number of clusters is determined by visualizing the average interval cluster values with respect to number of clusters. If there is a visual elbow in the relationship, the elbow point is the optimal point. However, it should be noted that there could be more than one or no elbow points. In this case, other mentioned methods should be performed to find the optimal value.

User clustering is the main focus of this work. However, intra-cluster power allocation that allows successful SIC is another essential step for NOMA applications. In the next chapter, implemented power allocation method is examined.

5. POWER ALLOCATION

In this work, the power allocation algorithm proposed in [8] is executed. The algorithm provides the optimal power allocation under several assumptions. Initially, $p_i = p_j$ is assumed for $\forall i, j \in \mathcal{K}$ to reduce the complexity of the power allocation problem. In other words, it only optimizes the intra-cluster power allocation. The equivalent channel gain of user $\pi_k(j)$ is calculated by

$$g_{k,\pi_k(j)} = \frac{|\mathbf{h}^H_{\psi(k),\pi_k(j)}\mathbf{w}_{\psi(k),k}|^2 p_k}{\sum_{l\neq k}|\mathbf{h}^H_{\psi(l),\pi_k(j)}\mathbf{w}_{\psi(l),l}|^2 p_l + \sigma^2}. \tag{5.1}$$

Then, the optimal decoding order of k-th cluster is determined such that

$$g_{k,\pi_k(1)} \leq g_{k,\pi_k(2)} \leq \cdots \leq g_{k,\pi_k(L_k)}. \tag{5.2}$$

The SINR of user $\pi_k(j)$ can be rearranged into the following formula by considering (2.11), (5.1) and (5.2)

$$\Gamma_{k,\pi_k(j)} = \frac{\beta_{k,\pi_k(j)} g_{k,\pi_k(j)}}{1 + g_{k,\pi_k(j)} \sum_{i>j} \beta_{k,\pi_k(i)}}. \tag{5.3}$$

By using this assumptions, the optimization problem to maximize the system output while guaranteeing the QoS constraint of minimum sum rate per user can be expressed as

$$\max_{\beta_{\mathbf{k}},\pi_{\mathbf{k}}} \quad \sum_{j=1}^{L_k} \log(1 + \Gamma_{k,\pi_k(j)}) \tag{5.4a}$$

$$\text{s.t.} \quad \sum_{u=1}^{L_k} \beta_{k,u} = 1,\ k \in \mathcal{K}, \tag{5.4b}$$

$$\Gamma_{k,\pi_k(j)} \geq \bar{\Gamma}_{k,\pi_k(j)},\ \pi_k(j) \in \mathcal{C}_k, k \in \mathcal{K}. \tag{5.4c}$$

$\boldsymbol{\beta}_k$, intra-cluster power allocation coefficient vector of cluster k can be divided into two parts as $\boldsymbol{\beta}_k = \bar{\boldsymbol{\beta}}_k + \tilde{\boldsymbol{\beta}}_k$. $\bar{\boldsymbol{\beta}}_k$ denotes the minimum intra-cluster power allocation coefficient vector of the cluster k. $\tilde{\boldsymbol{\beta}}_k$ denotes the excess intra-cluster power allocation coefficient vector of the cluster k.

Proposition 5.1. *[8]*

(i) The problem stated in (5.4) *is feasible if*

$$\bar{\beta}_k \triangleq \sum_{j=1}^{L_k} [\prod_{i=1}^{j-1} (1 + \bar{\Gamma}_{k,\pi_k(i)})] \frac{\bar{\Gamma}_{k,\pi_k(j)}}{g_{k,\pi_k(j)}} \leq 1, \tag{5.5}$$

where the power allocation vector $\mathbf{p}$ *and beamforming vectors are given.*

(ii) If the problem is feasible, the optimal objective value U^* *can be expressed as*

$$U^* = \bar{U} + \log(1 + \frac{(1 - \bar{\beta}_k) g_{k,\pi_k(L_k)}}{\prod_{i \leq L_k} (1 + \bar{\Gamma}_{k,\pi_k(L_k)})}). \tag{5.6}$$

The corresponding power splitting factors for NOMA can be expressed as

$$\beta_{k,\pi_k(j)} = \bar{\beta}_{k,\pi_k(j)} + \tilde{\beta}_{k,\pi_k(j)}, \tag{5.7}$$

where $\bar{\beta}_{k,\pi_k(j)}$ *denotes the minimum intra-cluster power allocation coefficient for user* $\pi_k(j)$ *to satisfy the targeted* $\bar{\Gamma}$*. On the other hand,* $\tilde{\beta}_{k,\pi_k(L_k)}$ *is used to increase the rate of user* $\pi_k(L_k)$ *to maximize the system output. Additionally,* $\tilde{\beta}_{k,\pi_k(j)}, \forall j < L_k$ *compensates the SINR loss due to the extra intra-cluster interference caused by* $\tilde{\beta}_{k,\pi_k(L_k)}$*. The power splitting factors are calculated by*

$$\bar{\beta}_{k,\pi_k(j)} = \frac{\bar{\Gamma}_{k,\pi_k(j)}}{g_{k,\pi_k(j)}} + \bar{\Gamma}_{k,\pi_k(j)} \sum_{i>j} \bar{\beta}_{k,\pi_k(i)} \tag{5.8}$$

$$\tilde{\beta}_{k,\pi_k(j)} = \begin{cases} \bar{\Gamma}_{k,\pi_k(j)} \sum_{i>j} \tilde{\beta}_{k,\pi_k(i)}, & \text{if } j < L_k \\ \frac{1-\bar{\beta}_k}{\prod_{i<L_k} (1+\bar{\Gamma}_{k,\pi_k(i)})}, & \text{if } j = L_k \end{cases} \tag{5.9}$$

Proof. See Appendix B of [8]. □

As the final assumption, $\bar{\Gamma}_{k,\pi_k(i)} = \bar{\Gamma}_{k,\pi_k(j)} = \bar{\Gamma}, \forall \pi_k(i), \pi_k(j) \in \mathcal{C}_k, \forall k \in \mathcal{K}$ is presumed to further simply the calculations. In the next chapter, simulation results will be demonstrated.

6. SIMULATION RESULTS

A simulation environment is prepared by using Python 3.7.4 programming language [25] in Spyder 4.0.0rc1 integrated development environment (IDE) [26]. The system model and the implemented techniques explained in previous chapters are programmed by using the following python libraries: numpy 1.16.5 [27], pandas 0.25.1 [28], scikit-learn 0.21.3 [29], matplotlib 3.1.1 [30], pyclustering 0.9.3.1 [31] and scipy 1.3.1 [32].

For all simulations, the noise power and the SINR threshold for all users are assumed $\sigma^2 = -30$ dBm and $\bar{\Gamma} = 0.02$ dB, respectively.

Although this work mainly focuses on multi cellular scenario with multiple base stations, starting evaluations with a single cell scenario is helpful to understand the effect of intra-cell interference on the system performance without any inter-cluster interference. Additionally, the effect of each parameter on the intra-cell interference may be understood in a better way by examining them separately.

In Figure 6.1, the effect of L_k in single beam millimeter wave NOMA systems is investigated. To be able to do so, one cluster with varying L_k is considered. Transmission power is set to 35 dB. Number of base stations, number of antennas, radius of coverage, radius of children distribution are assumed $B = 1$, $M = 4$, $R = 5$ m and $r = 1$ m, respectively. As it can be observed from the figure, the overall OMA sum rate stays constant with varying values of L_k. This is because all users use the same beam with the same power domain resources. On the other hand, the increase in number of users also increases the overall system output in NOMA case. However, the increase is restricted in terms of maximum number of users by the transmission power in a NOMA system since it utilizes the power domain. Intra-cluster interference is worsen by the addition of each new user. Increase in the transmission power is required in order to be able to overcome it and to satisfy the specified minimum QoS conditions.

Consequently, the increase follows the law of diminishing returns as it can also be observed from the Figure 6.1. Users should be clustered so that there would be an upper limit to number of users and it should be as optimal as possible in order to fully benefit from NOMA. Otherwise, implementation of NOMA could fail due to intra-cluster interference. If there are too many users in the same DoF, they could be clustered into smaller clusters that communicate via NOMA in different subcarriers. This is called Multicarrier NOMA (MC-NOMA). For the rest of the simulations except Figure 6.8, number of users per clusters is assumed constant with a value such that NOMA power allocation can be performed successfully within the transmission power limits.

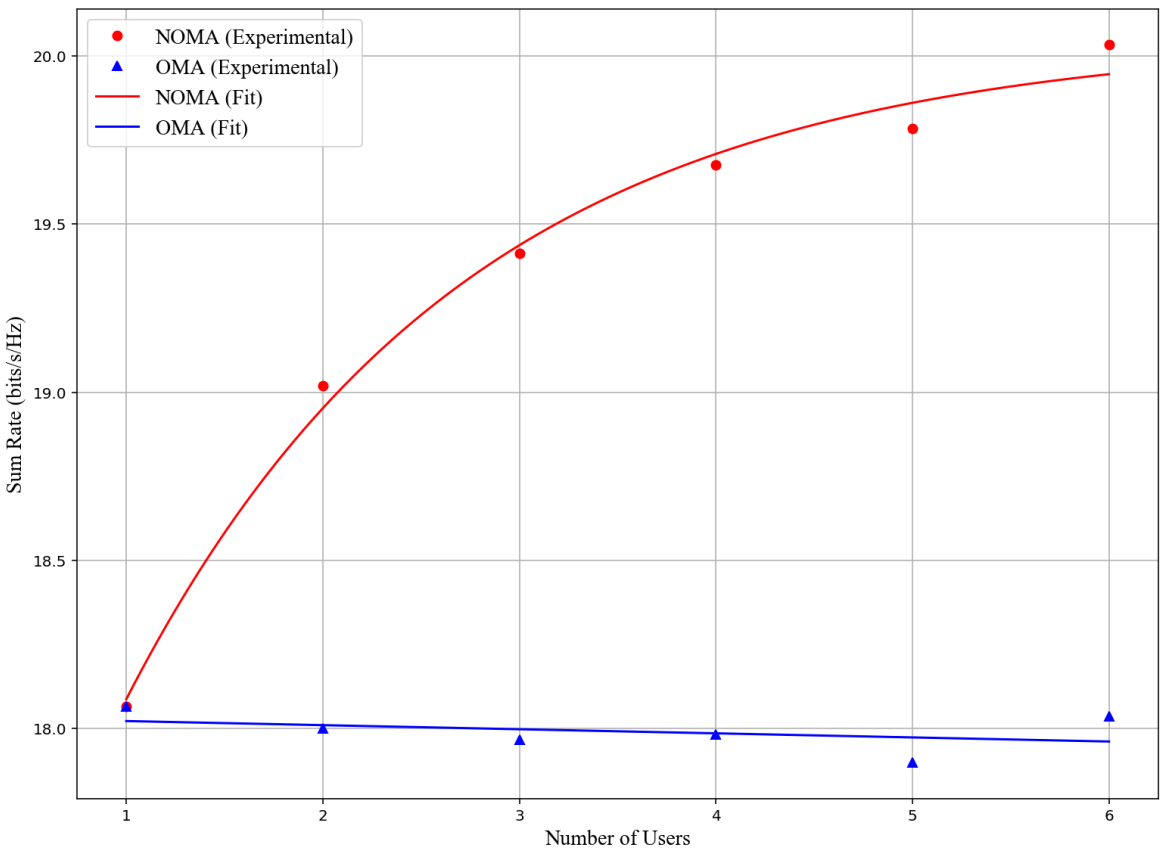

Figure 6.1. Effect of L_k to Sum Rate.

In Figure 6.2, the effect of M in single beam millimeter wave NOMA systems is examined. Therefore, one cluster with varying M is considered. Transmission power is set to 30 dB. Number of base stations, number of users, radius of coverage, radius of children distribution are assumed $B = 1$, $U = 4$, $R = 5$ m and $r = 1$ m, respectively. The overall system output increases for both NOMA and OMA cases as expected due to the better spectral efficiency. It can be concluded that the number of antennas does not provide any advantage for NOMA over OMA when there is no inter-cluster interference, since the increase is in similar proportions for both of the cases.

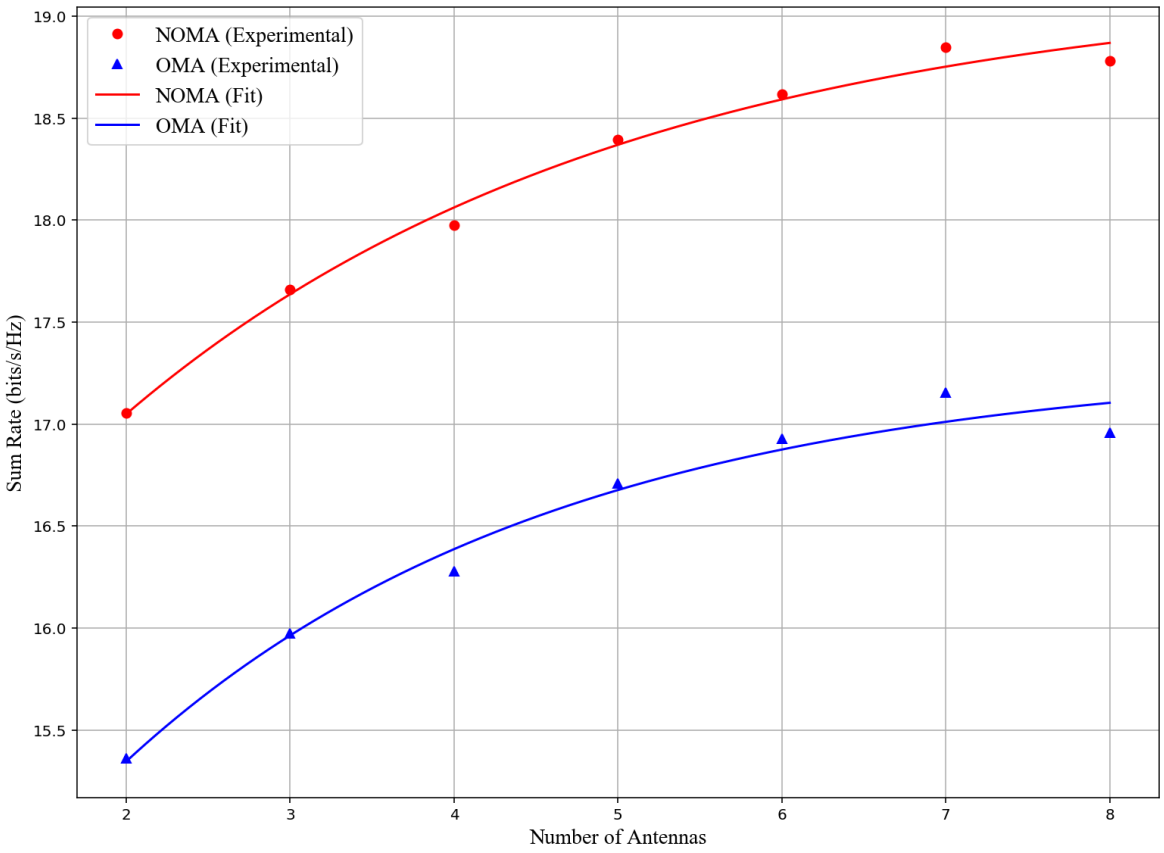

Figure 6.2. Effect of M to Sum Rate.

Transmission power directly affects the signal power and the interference power. Therefore, it is a significant factor in SINR and channel capacity. In Figure 6.3, the effect of P in single beam millimeter wave NOMA systems is investigated.

Consequently, one cluster with varying P is considered. Number of base stations, number of users, number of antennas, radius of coverage, radius of children distribution are assumed $B = 1$, $U = 4$, $M = 4$, $R = 5$ m and $r = 1$ m, respectively. As it can be observed from the figure, the overall sum rates in both schemes increase logarithmically with varying values of P. The reason is that there is no inter-cluster interference to restrict SINR and the sum rate growth in a single beam millimeter wave NOMA system. It can be concluded that the transmission power does not provide any advantage for NOMA over OMA when there is no inter-cluster interference, since the increase is in similar proportions for both of the cases. In NOMA, the increase only benefits the user with the best channel condition contrary to OMA where it benefits all of the users.

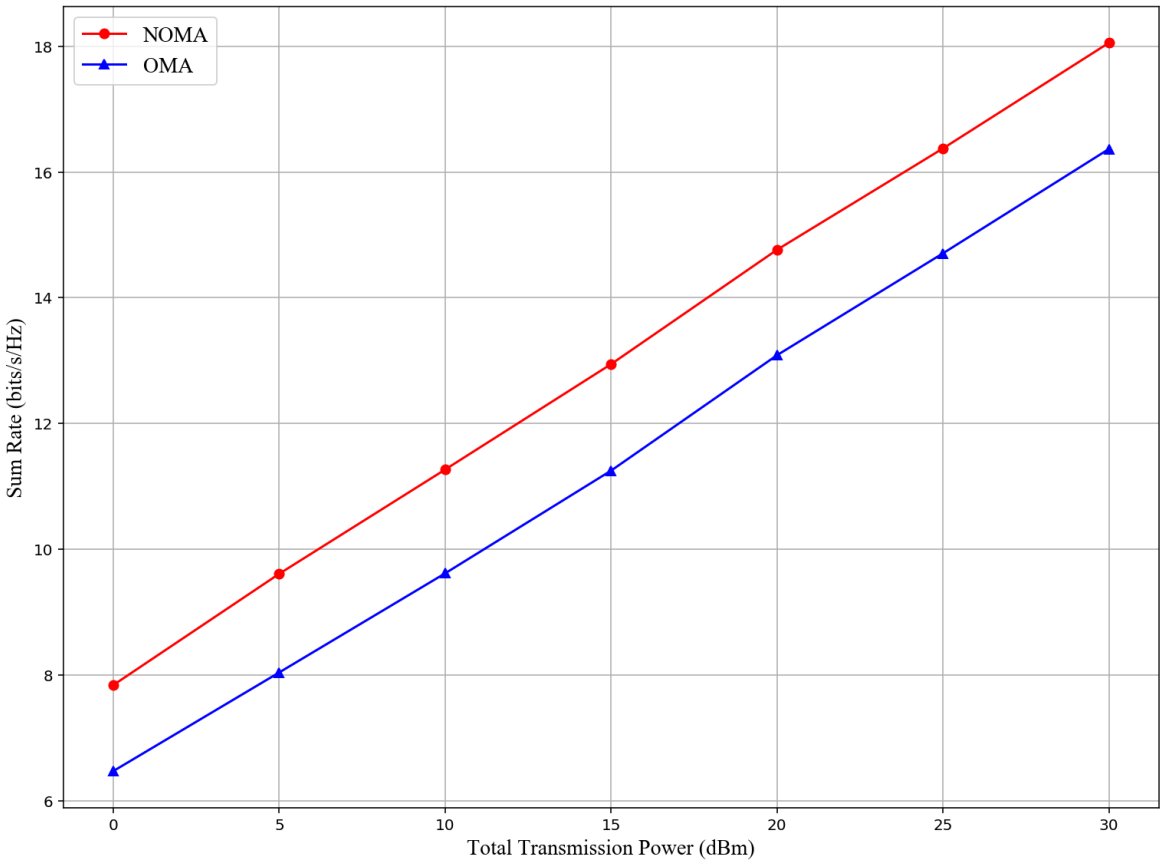

Figure 6.3. Effect of P to Sum Rate.

For the scenarios with more than one cluster, user clustering is the first step as mentioned in Section 4. A simulation is deployed with the presumptions that number of users, number of base stations, number of clusters, number of base station antennas, radius of coverage and radius of children are $U = 45$, $B = 3$, $K = 3$, $M = 6$, $R = 5$ m, $R_k = 0.5$ m, respectively. The AoD for parent points distributed such that they would be inside of the equilateral triangle between the base stations. A sample distribution can be observed in Figure 6.4. The first thing to determine before running the K-medoids algorithm is the feature vector. As mentioned in Chapter 4, AoD's to each base station can be used as a single feature, which sums up to three features per user since three base stations are used in the simulation. Although this would need the base stations to share CSI of all users between each other and increase the backhaul complexity, it is not included in the scope of this work. Additionally, perfect knowledge of users' CSI is assumed.

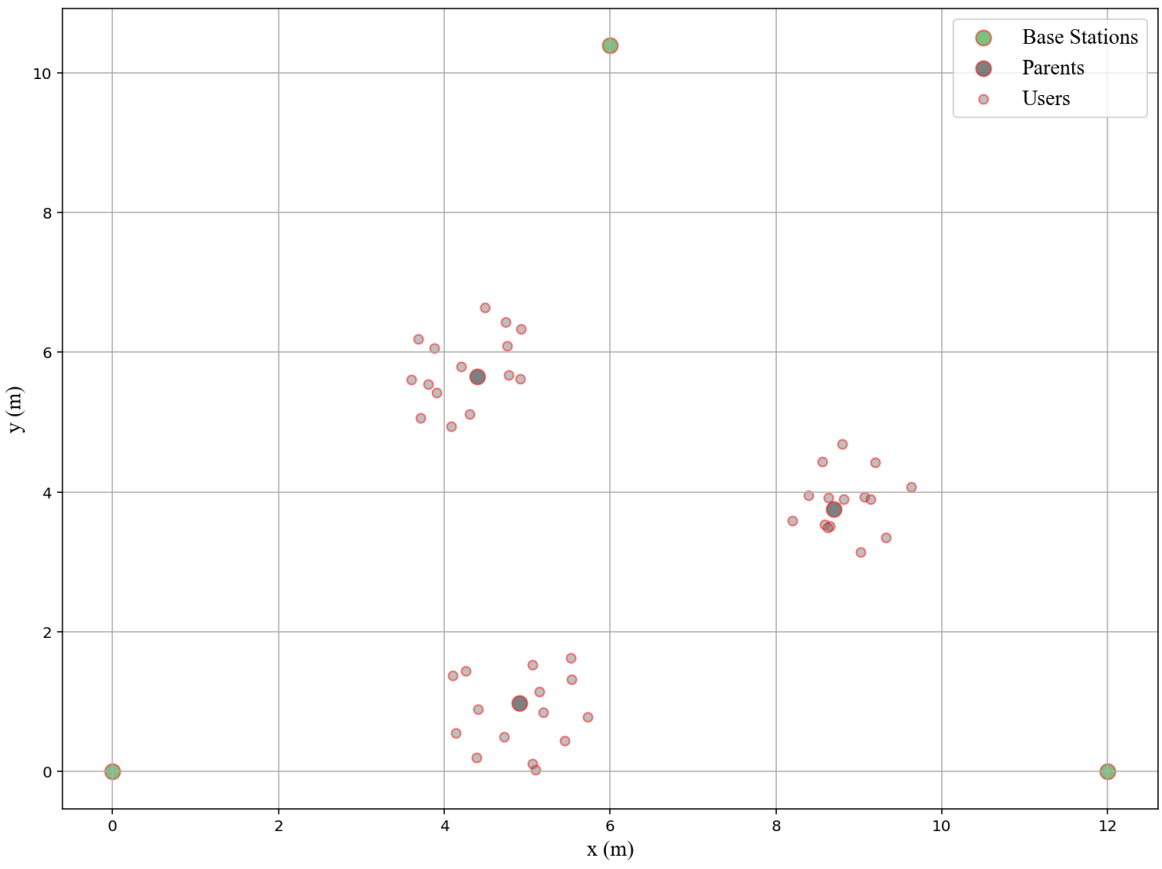

Figure 6.4. Spatial Distribution.

The second step is executing the elbow method due to the assumption of not knowing the exact number of clusters. Although this would require the algorithm to run for multiple times, it is a simple method to find the optimal point. The Figure 6.5 demonstrates the elbow method by calculating the average internal cluster distance by using (4.2) for varying number of clusters. It forms the elbow point on $K = 3$.

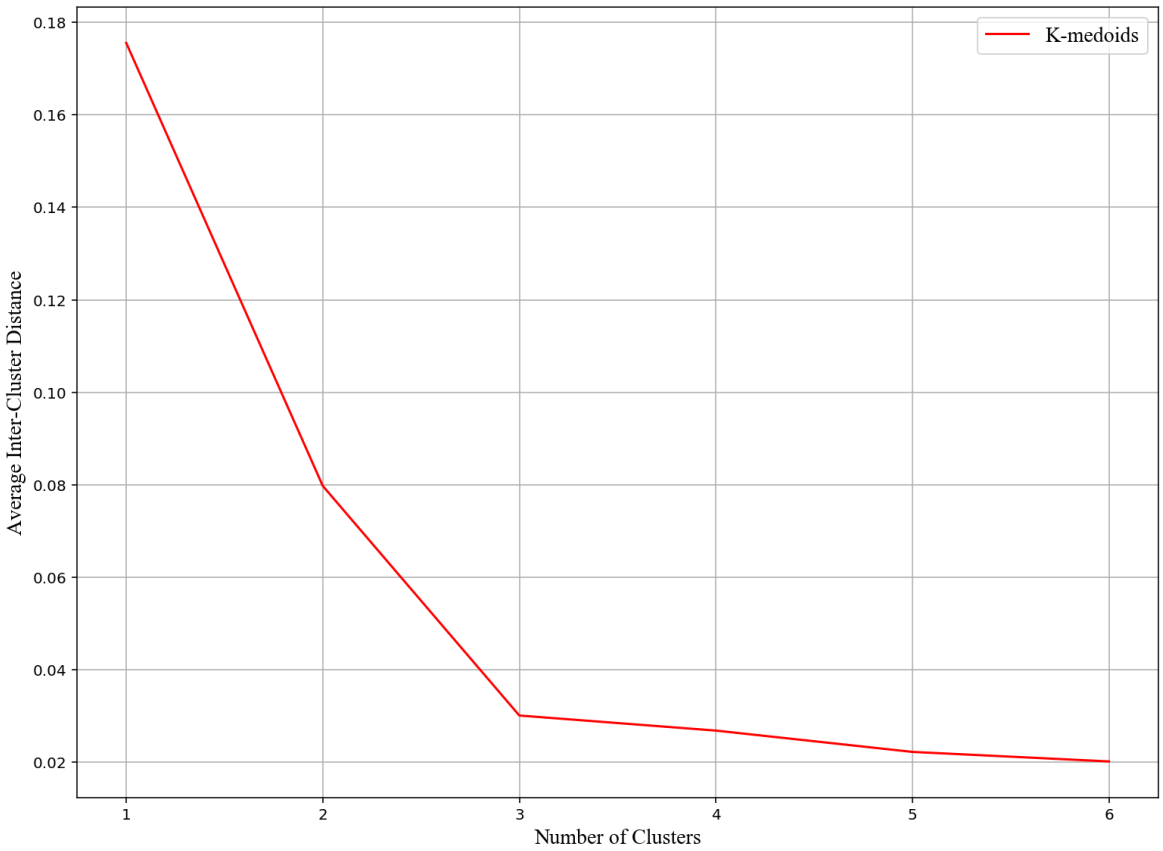

Figure 6.5. Elbow Method.

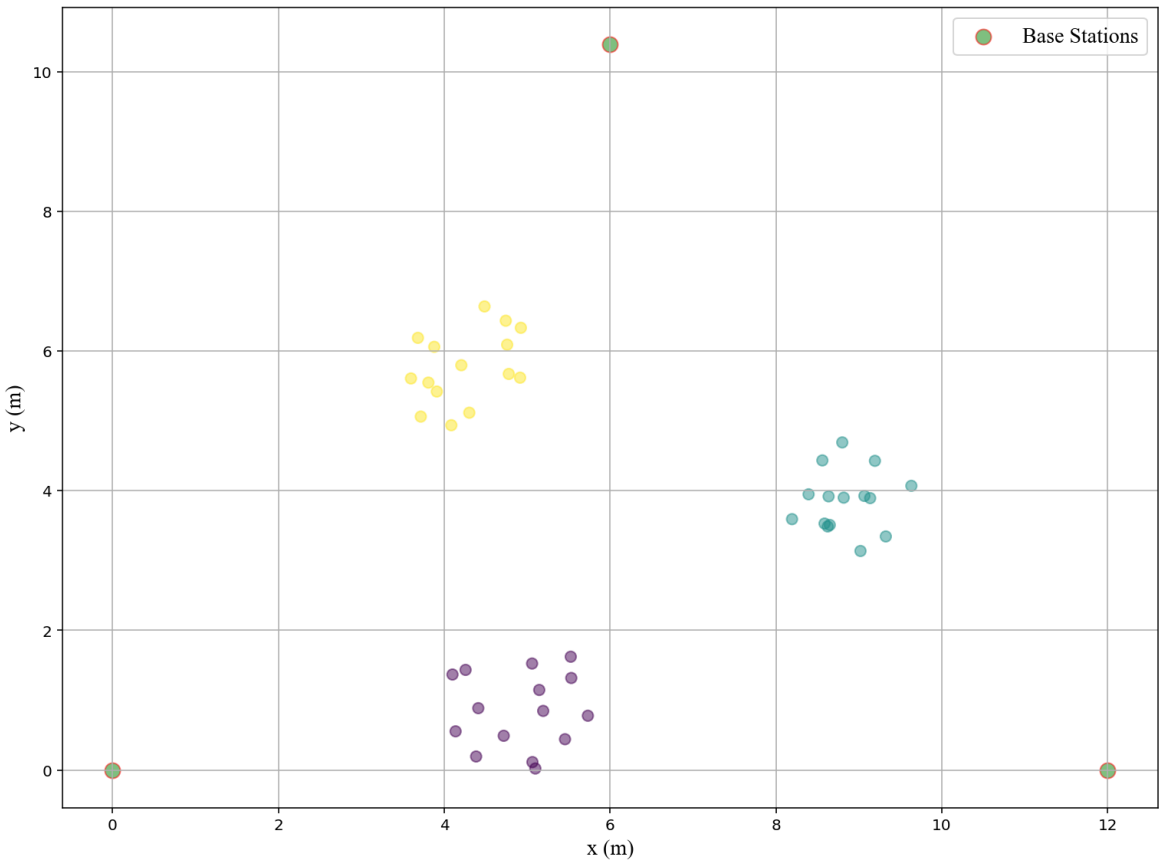

Figure 6.6. Illustration of K-Medoids User Clustering.

Figure 6.6 displays user clustering using the K-medoids based algorithm on the elbow point, $K = 3$. Different clusters are colored in different colors in the figure. It clusters the users perfectly as it can be easily observed.

In Figure 6.7, the effect of M in millimeter wave NOMA systems is investigated. To be able to do so, varying M is considered. Transmission power is set to 30 dB. Number of base stations, number of clusters, number of users, radius of coverage, radius of children distribution are assumed $B = 2$, $K = 2$, $U = 4$, $R = 5$ m and $r = 1$ m, respectively. The overall system output increases for both NOMA and OMA cases as expected due to the better spectral efficiency.

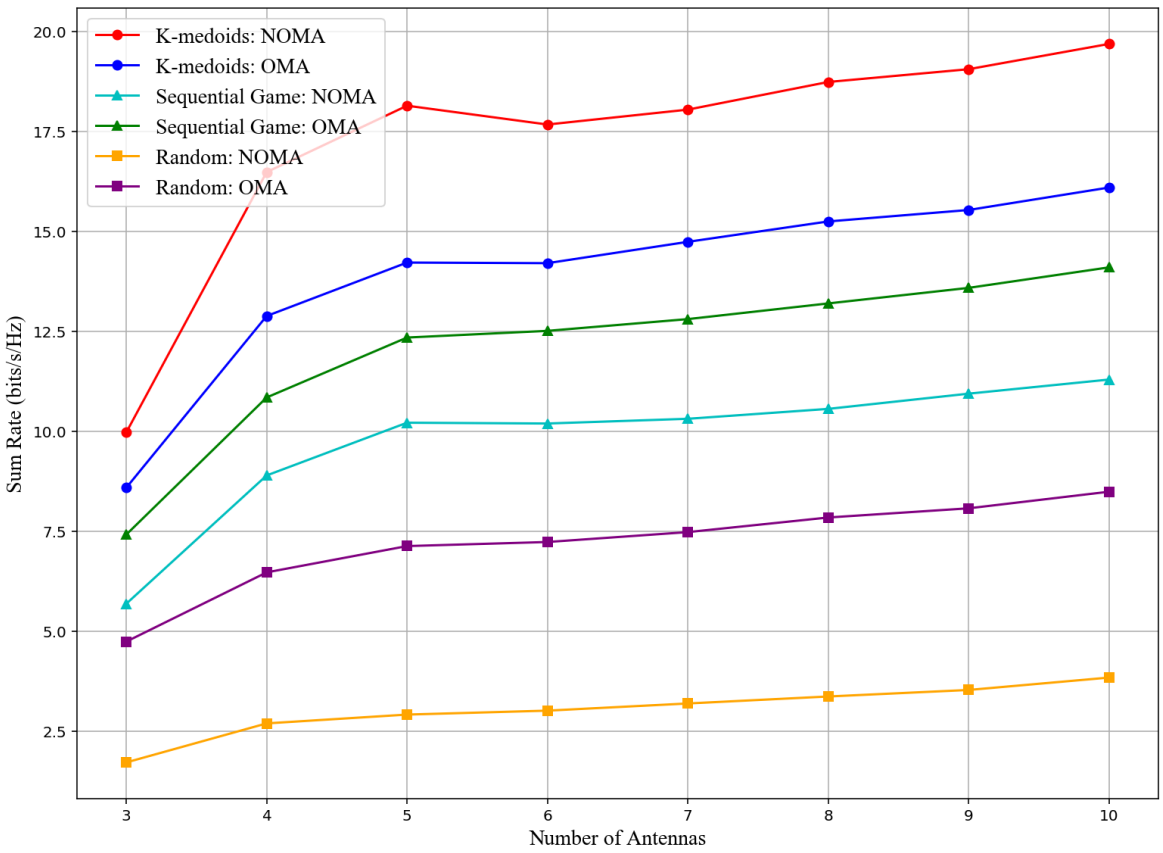

Figure 6.7. Effect of M to Sum Rate.

In Figure 6.8, the effect of L_k in millimeter wave NOMA systems is investigated. To be able to do so, varying L_k is considered. Transmission power is set to 30 dB. Number of base stations, number of antennas, number of clusters, radius of coverage, radius of children distribution are assumed $B = 2$, $M = 6$, $K = 2$, $R = 5$ m and $r = 1$ m, respectively. As it is expected, the overall OMA sum rate of K-medoids based user clustering stays constant with varying values of L_k. On the other hand, this is not the case for the random clustering since poor clustering causes higher inter cluster interference. It can be observed that NOMA performs better than OMA only in K-medoids clustering. However, NOMA sum rate also stays constant with varying values of L_k in contrast to the increase observed in the case with single cell.

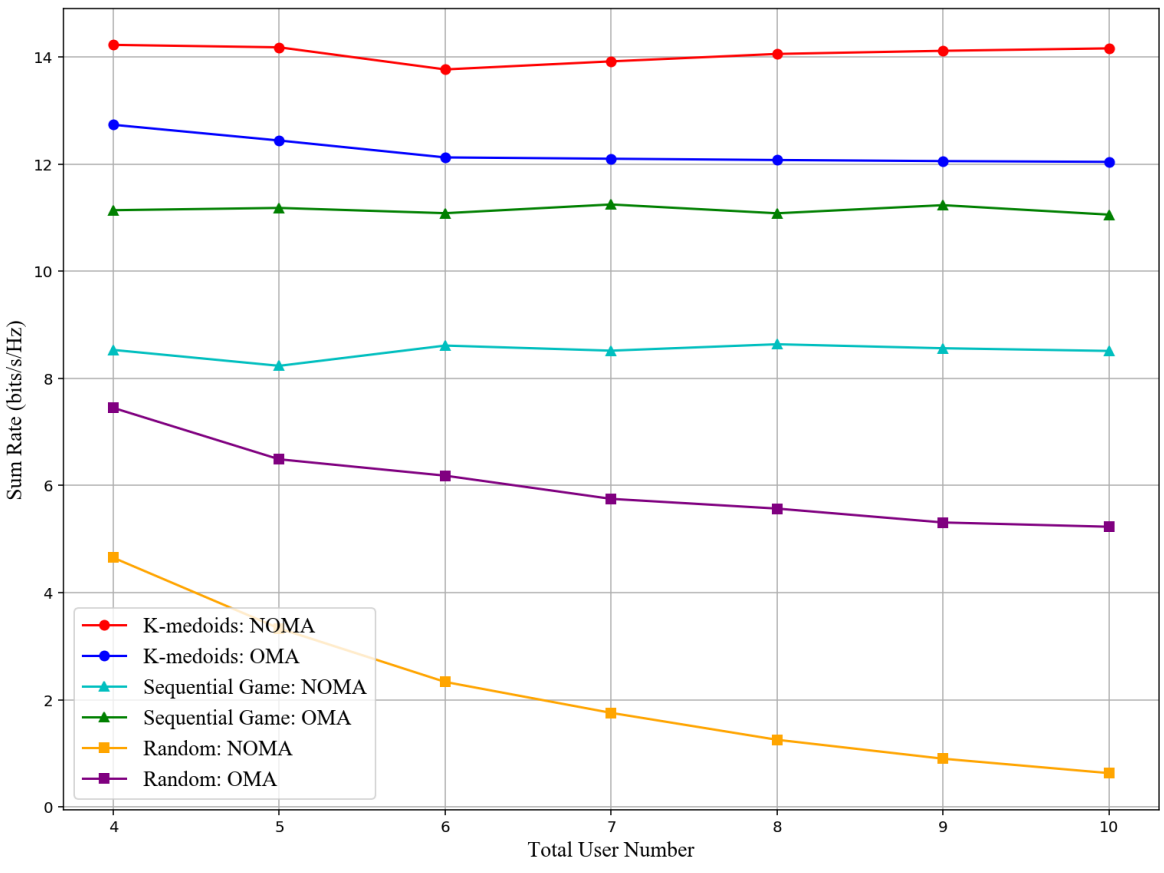

Figure 6.8. Effect of L_k to Sum Rate.

In Figure 6.9, the effect of P in millimeter wave NOMA systems is investigated. To be able to do so, varying P is considered. Number of base stations, number of users, number of antennas, number of clusters, radius of coverage, radius of children distribution are assumed $B = 2$, $U = 8$, $M = 4$, $K = 2$, $R = 5$ m and $r = 1$ m, respectively. The system output is compared in Figure 6.9 in two aspects. Firstly, it compares NOMA against OMA. NOMA performs better in only K-medoids user clustering. It demonstrates the significance of user clustering to the performance of NOMA systems. Secondly, it compares K-medoids user clustering against sequential game based and random user clustering methods. As expected, K-medoids user clustering achieves better sum rates in both NOMA and OMA since aligning beam with clusters to dismiss interference is an important aspect of millimeter wave communications and K-medoids provides better performance. Random user clustering in NOMA performs the worst of three since severe interference sabotages intra-cluster power allocation.

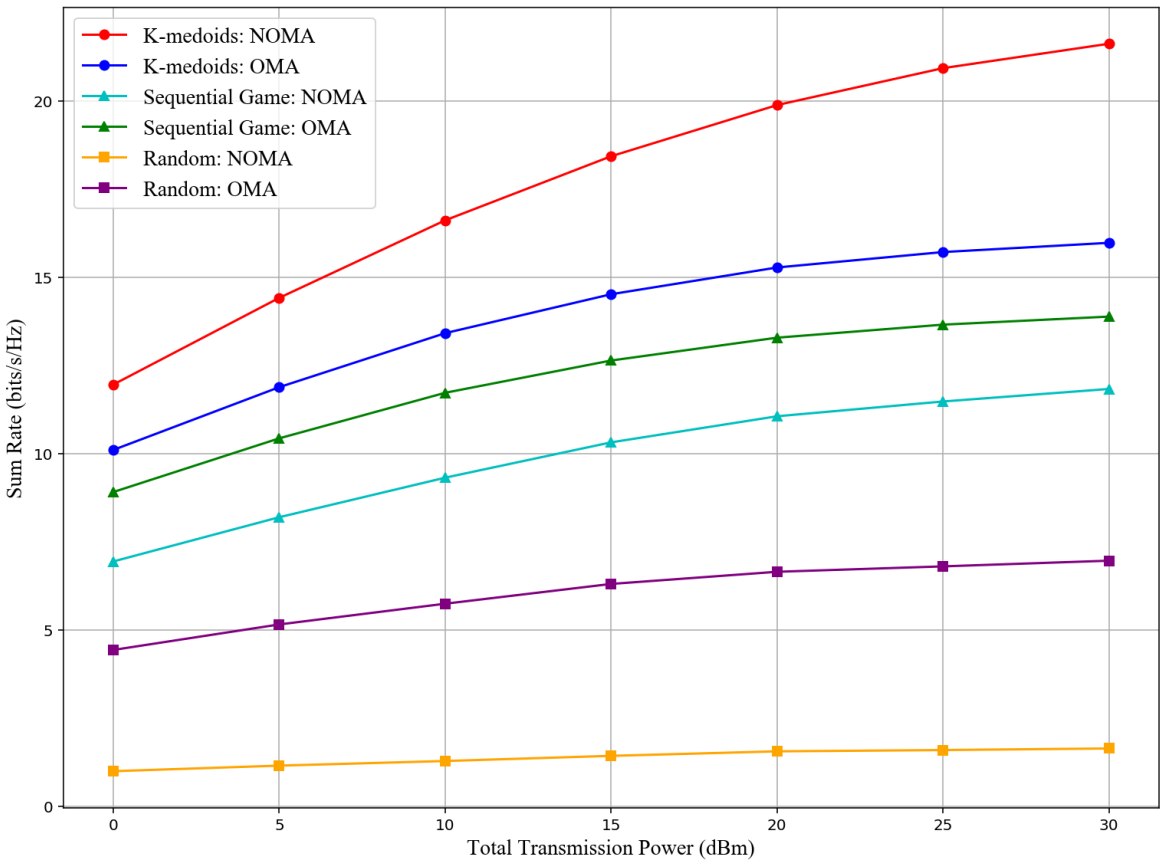

Figure 6.9. Effect of P to Sum Rate.

In Figure 6.10, the effect of CSI in millimeter wave NOMA systems is investigated. To be able to do so, varying P is considered for different CSI values. Number of base stations, number of users, number of antennas, number of clusters, radius of coverage, radius of children distribution are assumed $B = 2$, $U = 8$, $M = 4$, $K = 2$, $R = 5$ m and $r = 1$ m, respectively. It concludes that the K-medoids based user clustering algorithm is sensitive to the CSI accuracy. The negative effect of CSI imperfection can be diminished by optimizing features and distance functions.

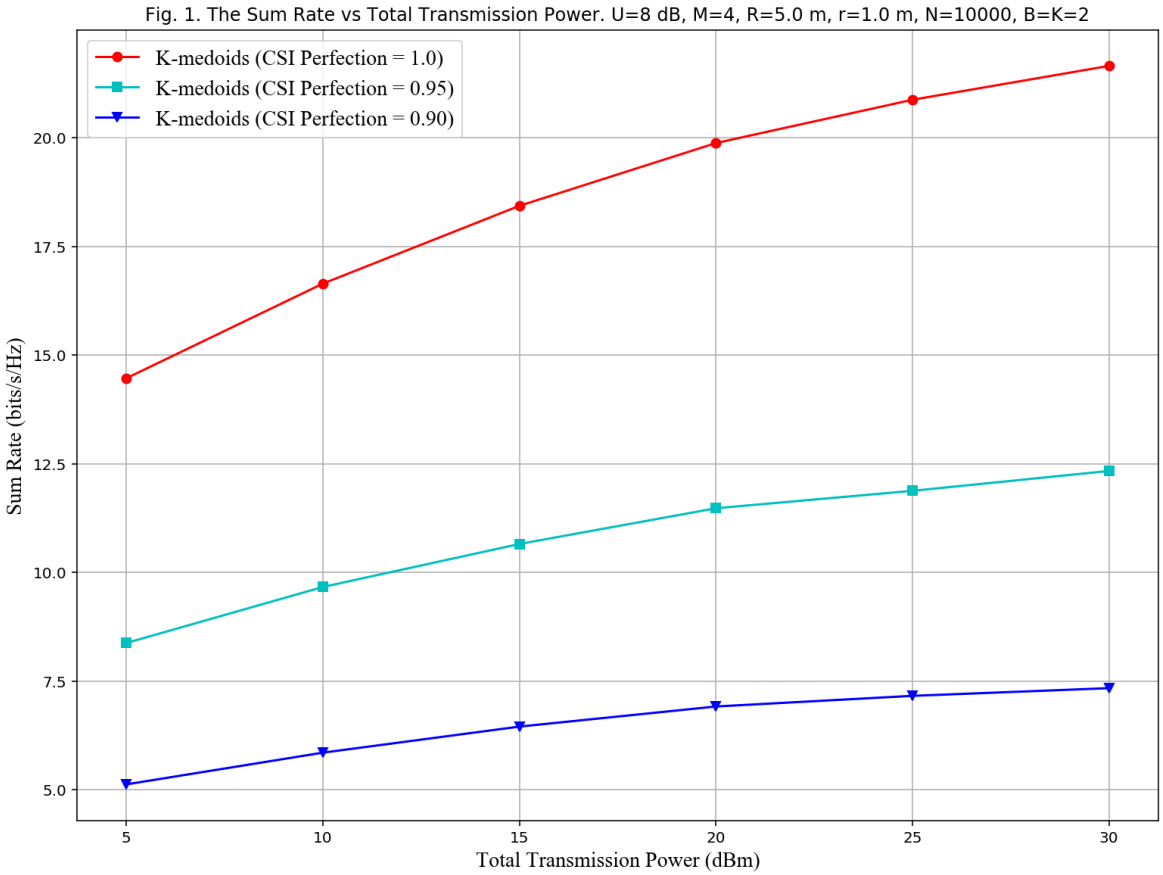

Figure 6.10. Effect of CSI to Sum Rate.

7. CONCLUSION AND FUTURE WORK

In this work, user clustering is investigated in downlink millimeter wave NOMA systems with intercell interference. The aim is to cluster users such that the system output under a certain QoS constraint is maximized. The users are distributed in a physically clustered way. Consequently, the way to achieve the goal is to cluster users such that users with correlated channels would be in the same cluster. A K-medoids based user clustering algorithm is proposed. Initially, the number of clusters is determined by using the elbow method and it is shown that the K-medoids based algorithm successfully clusters the users. The simulation results show that K-medoids provides higher system output than random user clustering and sequential game based user clustering by diminishing the intercell interference. Furthermore, the system performance is enhanced in NOMA over OMA only with the K-medoids based user clustering method. It demonstrates the significance of a successful user clustering on NOMA performance.

In this work, no beam interference suppression method for multi cellular systems is implemented. It allows us to evaluate the system performance of user clustering methods in isolation. However, a system with no additional beam interference suppression method requires a low complexity clustering problem to be able to successfully execute SIC. In a simulation with initially physically clustered users, most of the unsupervised clustering methods perform similarly in terms of user clustering and the system output. In this case, the only comparison between them is in terms of complexity. Therefore, a possible step in future is to implement additional methods to diminish the intercell interference in a downlink millimeter wave NOMA system with a more complex user distribution. Consequently, unsupervised clustering methods can be compared distinctively in terms the system output.

On the other hand, power allocation is another important factor on SIC and NOMA performance. In this work, inter-cluster and intra-cluster power allocations are handled separately. The inter-cluster power allocation is simply equally distributed.

As a future work, a sum rate maximization problem that handles inter-cluster power allocation jointly with intra-cluster power allocation and user clustering can be developed and solved. Consequently, the downlink millimeter wave NOMA system performance and fairness can be improved further.

REFERENCES

1. Busari, S. A., K. M. S. Huq, S. Mumtaz, L. Dai and J. Rodriguez, "Millimeter-Wave Massive MIMO Communication for Future Wireless Systems: A Survey", *IEEE Communications Surveys & Tutorials*, Vol. 20, No. 2, pp. 836–869, 2018.

2. Xiao, M., S. Mumtaz, Y. Huang, L. Dai, Y. Li, M. Matthaiou, G. K. Karagiannidis, E. Björnson, K. Yang, C. I and A. Ghosh, "Millimeter Wave Communications for Future Mobile Networks", *IEEE Journal on Selected Areas in Communications*, Vol. 35, No. 9, pp. 1909–1935, 2017.

3. Lee, G., Y. Sung and J. Seo, "Randomly-Directional Beamforming in Millimeter-Wave Multiuser MISO Downlink", *IEEE Transactions on Wireless Communications*, Vol. 15, No. 2, pp. 1086–1100, 2016.

4. Zheng, L. and D. N. C. Tse, "Diversity and multiplexing: a fundamental tradeoff in multiple-antenna channels", *IEEE Transactions on Information Theory*, Vol. 49, No. 5, pp. 1073–1096, 2003.

5. Goldsmith, A., *Wireless Communications*, Cambridge University Press, USA, 2005.

6. Wang, X., L. Kong, F. Kong, F. Qiu, M. Xia, S. Arnon and G. Chen, "Millimeter Wave Communication: A Comprehensive Survey", *IEEE Communications Surveys & Tutorials*, Vol. 20, No. 3, pp. 1616–1653, 2018.

7. Wang, K., J. Cui, Z. Ding and P. Fan, "Stackelberg Game for User Clustering and Power Allocation in Millimeter Wave-NOMA Systems", *IEEE Transactions on Wireless Communications*, Vol. 18, No. 5, pp. 2842–2857, 2019.

8. Cui, J., Z. Ding, P. Fan and N. Al-Dhahir, "Unsupervised Machine Learning-Based User Clustering in Millimeter-Wave-NOMA Systems", *IEEE Transactions*

on Wireless Communications, Vol. 17, No. 11, pp. 7425–7440, 2018.

9. Ren, J., Z. Wang, M. Xu, F. Fang and Z. Ding, "An EM-Based User Clustering Method in Non-Orthogonal Multiple Access", *IEEE Transactions on Communications*, Vol. 67, No. 12, pp. 8422–8434, 2019.

10. Cui, J., M. B. Khan, Y. Deng, Z. Ding and A. NaIlanathan, "Unsupervised Learning Approaches for User Clustering in NOMA enabled Aerial SWIPT Networks", *2019 IEEE 20th International Workshop on Signal Processing Advances in Wireless Communications (SPAWC)*, pp. 1–5, 2019.

11. Zhang, Z. and H. Yu, "Beam interference suppression in multi-cell millimeter wave communications", *Digital Communications and Networks*, Vol. 5, January 2018.

12. Shao, W., S. Zhang, H. Li, N. Zhao and O. A. Dobre, "Angle-Domain NOMA Over Multicell Millimeter Wave Massive MIMO Networks", *IEEE Transactions on Communications*, Vol. 68, No. 4, pp. 2277–2292, 2020.

13. Xue, Q., X. Fang, M. Xiao and L. Yan, "Multiuser Millimeter Wave Communications With Nonorthogonal Beams", *IEEE Transactions on Vehicular Technology*, Vol. 66, No. 7, pp. 5675–5688, 2017.

14. Chen, Z., Z. Ding, X. Dai and G. K. Karagiannidis, "On the Application of Quasi-Degradation to MISO-NOMA Downlink", *IEEE Transactions on Signal Processing*, Vol. 64, No. 23, pp. 6174–6189, 2016.

15. Alkhateeb, A., G. Leus and R. W. Heath, "Limited Feedback Hybrid Precoding for Multi-User Millimeter Wave Systems", *IEEE Transactions on Wireless Communications*, Vol. 14, No. 11, pp. 6481–6494, 2015.

16. Zhang, D., Z. Zhou, C. Xu, Y. Zhang, J. Rodriguez and T. Sato, "Capacity Analysis of NOMA With mmWave Massive MIMO Systems", *IEEE Journal on Selected Areas in Communications*, Vol. 35, No. 7, pp. 1606–1618, 2017.

17. Ding, Z., P. Fan and H. V. Poor, "Random Beamforming in Millimeter-Wave NOMA Networks", *IEEE Access*, Vol. 5, pp. 7667–7681, 2017.

18. Lapidoth, A. and S. Shamai, "Fading channels: how perfect need "perfect side information" be?", *IEEE Transactions on Information Theory*, Vol. 48, No. 5, pp. 1118–1134, 2002.

19. Sumathi, S. and A. Thakre, "Impact of Imperfect Channel State Information on Downlink Sum-Rate of Two user mmWave Non Orthogonal Multiple Access", *2019 International Conference on Communication and Electronics Systems (ICCES)*, pp. 1–6, 2019.

20. T, V. and S. T, "Computational Complexity between K-Means and K-Medoids Clustering Algorithms for Normal and Uniform Distributions of Data Points", *Journal of Computer Science*, Vol. 6, 2010.

21. Kaufman, L. and P. J. Rousseeuw, "Clustering by Means of Medoids", Y. Dodge (Editor), *Statistical Data Analysis Based on the L1-norm and Related Methods*, pp. 405–416, Elsevier Science Pub. Co., Amsterdam, 1987.

22. Park, H. and C. Jun, "A simple and fast algorithm for K-medoids clustering", *Expert Systems with Applications*, Vol. 36, No. 2, pp. 3336–3341, 2009.

23. Schubert, E. and P. J. Rousseeuw, "Faster k-Medoids Clustering: Improving the PAM, CLARA, and CLARANS Algorithms", G. Amato, C. Gennaro, V. Oria and M. Radovanović (Editors), *Similarity Search and Applications*, pp. 171–187, Springer International Publishing, Cham, 2019.

24. Goutte, C., P. Toft, E. Rostrup, F. Å. Nielsen and L. K. Hansen, "On clustering fMRI time series", *NeuroImage*, Vol. 9, No. 3, pp. 298–310, 1999.

25. Rossum, G., *Python Reference Manual*, CWI (Centre for Mathematics and Computer Science), Amsterdam, The Netherlands, 1995.

26. Spyder Doc Contributors, *Spyder: The Scientific Python Development Environment — Documentation*, `https://docs.spyder-ide.org/`, accessed in May 2020.

27. NumPy Community, *NumPy Reference*, 1.16.6 edn., 2020, `https://numpy.org/doc/1.16/numpy-ref.pdf`, accessed in May 2020.

28. McKinney, W. and PyData Development Team, *pandas: powerful Python data analysis toolkit*, 0.25.1 edn., 2019, `https://pandas.pydata.org/pandas-docs/version/0.25.1/pandas.pdf`, accessed in May 2020.

29. Pedregosa, F., G. Varoquaux, A. Gramfort, V. Michel, B. Thirion, O. Grisel, M. Blondel, P. Prettenhofer, R. Weiss, V. Dubourg, J. Vanderplas, A. Passos, D. Cournapeau, M. Brucher, M. Perrot and E. Duchesnay, "Scikit-learn: Machine Learning in Python", *Journal of Machine Learning Research*, Vol. 12, pp. 2825–2830, 2011.

30. Hunter, J. D., "Matplotlib: A 2D graphics environment", *Computing in Science & Engineering*, Vol. 9, No. 3, pp. 90–95, 2007.

31. Novikov, A., "PyClustering: Data Mining Library", *Journal of Open Source Software*, Vol. 4, No. 36, p. 1230, 2019.

32. SciPy Community, *SciPy Reference Guide*, 1.3.0 edn., 2019, `https://docs.scipy.org/doc/scipy-1.3.0/scipy-ref-1.3.0.pdf`, accessed in June 2020.